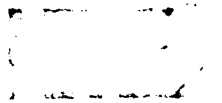




AD A107706

DTRC FILE COPY



12

TRW Document No. 35524-6002-UT-00  
ONR Contract N00014-79-C-0508  
October 1981

ANALYTIC MODELING OF SEVERE VORTICAL STORMS

Final Report  
9 July 1980 - 31 December 1981

by

Engineering Sciences Laboratory  
TRW Defense and Space Systems Group  
One Space Park  
Redondo Beach, California 90278  
Francis E. Fendell, Principal Investigator

for

Artic and Earth Sciences Division  
Office of Naval Research  
800 North Quincy Street  
Arlington, Virginia 22217  
Walter F. Martin, Scientific Officer,  
Director, Atmospheric & Ionospheric Sciences Program

NOV 1981  
A

This document has been approved  
for public release and sale; its  
distribution is unlimited.

Reproduction in whole or in part is permitted  
for any purpose of the United States Government.

UNCLASSIFIED

SECURITY CLASSIFICATION OF THIS PAGE (When Data Entered)

REPORT DOCUMENTATION PAGE		READ INSTRUCTIONS BEFORE COMPLETING FORM
1. REPORT NUMBER	2. GOVT ACCESSION NO.	3. RECIPIENT'S CATALOG NUMBER
	DD-A 304	706
4. TITLE (and Subtitle) Analytic Modeling of Severe Vortical Storms		5. TYPE OF REPORT & PERIOD COVERED Final Report 9 July 1980 - 31 Dec 1981
		6. PERFORMING ORG. REPORT NUMBER 35524-6002-UT-00
7. AUTHOR(s) George Carrier Francis Fendell Phillip Feldman		8. CONTRACT OR GRANT NUMBER(s) NG0014-79-C-0508
9. PERFORMING ORGANIZATION NAME AND ADDRESS TRW Defense and Space Systems Group One Space Park Redondo Beach, CA 92078		10. PROGRAM ELEMENT, PROJECT, TASK AREA & WORK UNIT NUMBERS
11. CONTROLLING OFFICE NAME AND ADDRESS Office of Naval Research 800 N. Quincy Street Arlington, VA 22217		12. REPORT DATE October 1981
		13. NUMBER OF PAGES 56
14. MONITORING AGENCY NAME & ADDRESS (if different from Controlling Office)		15. SECURITY CLASS. (of this report) Unclassified
		15a. DECLASSIFICATION/DOWNGRADING SCHEDULE
16. DISTRIBUTION STATEMENT (of this Report) Unclassified - Distribution Unlimited		
17. DISTRIBUTION STATEMENT (of the abstract entered in Block 20, if different from Report)		
18. SUPPLEMENTARY NOTES		
19. KEY WORDS (Continue on reverse side if necessary and identify by block number) hurricane severe vortical storm tropical cyclone typhoon		
20. ABSTRACT (Continue on reverse side if necessary and identify by block number) The analytic modeling of well-organized rotating convective storms is invoked to elucidate the evolution from a moderately intense one-cell vortex, characterized by low-level pressure deficits on the order of one percent of atmospheric pressure, to a very intense two-cell vortex, characterized by low-level pressure deficits on the order of ten percent of atmospheric pressure. The physical distinction between the two stages rests on the insertion of a dry, compressionally heated, nonrotating,		

DD FORM 1 JAN 73 1473 EDITION OF 1 NOV 65 IS OBSOLETE

UNCLASSIFIED

11 SECURITY CLASSIFICATION OF THIS PAGE (When Data Entered)

## 20. ABSTRACT (Cont'd.)

central downdraft of originally tropopause-level air in the transition to the more severe case. The quasisteady mature description of the thermohydrodynamic structure of each vortex is being developed, and then the conditions for transition from the moderately intense to the very intense vortex will be sought. The practical motivation is to make progress toward the highly desirable, but very formidable task of being able to anticipate which tropical storms or minimal hurricanes will evolve to supertyphoons.

With a description of the one-cell storm, believed adequate for present purposes, already available, description of the two-cell vortex is the current challenge. In particular, since the potential-vortex and surface-inflow subdivisions of the structure of a very intense vortex are in hand, a realistic picture of the updraft and its location are sought.

The modeling proceeds from basic thermohydrodynamic principles. Nonessential geometric detail, as well as association of conclusions with the details of particular parameterizations, is being avoided as much as possible.

Tentative results achieved thus far, by an integral-type treatment that seeks the location of the eye wall and its properties with height, point to a particularly sensitive dependence on the vertical variation of the angular momentum in the portion of the vortex outside the eye wall. Perhaps for only certain, narrowly defined stratifications of angular momentum may the conservation laws be compatible with two-cell structure for an intense atmospheric vortex.

A

## TABLE OF CONTENTS

	<u>Page</u>
PREFACE	1
SUMMARY	2
1. INTRODUCTION	3
1.1 Statement of the Objective	3
1.2 An Approach to Two-Cell Structure for an Intense Atmosphere Vortex	4
1.3 The Boundary-Value Problem	5
2. A BOUNDARY-VALUE PROBLEM FOR THE TURNAROUND	7
3. TREATMENT OF A LOW-LEVEL SEPARATED LAYER WITHOUT STRUCTURE	12
4. A ONE-LAYER TREATMENT OF THE EYE WALL	19
5. PRELIMINARY RESULTS	31
6. FUTURE DIRECTIONS	34
TABLE	37
FIGURES	38
REFERENCES	49
APPENDIX A. A DERIVATION OF THE MOIST ADIABAT	51

## PREFACE

The participants in this program are Francis Fendell, principal investigator, and Phillip Feldman, numerical analyst, of TRW Defense and Space Systems Group, and George Carrier of Harvard University, Cambridge, MA, consultant to TRW. Also contributing was Paul Dergarabedian of the senior staff of the Energy Systems Division of TRW, now retired.

The participants are grateful to project technical monitors Walter Martin and James Hughes of the Atmospheric Sciences Program of the Office of Naval Research for their encouragement and their patience.

The manuscript was edited and typed by Lauren Hall.

## SUMMARY

The analytic modeling of well-organized rotating convective storms is invoked to elucidate the evolution from a moderately intense one-cell vortex, characterized by low-level pressure deficits on the order of one percent of atmospheric pressure, to a very intense two-cell vortex, characterized by low-level pressure deficits on the order of ten percent of atmospheric pressure. The physical distinction between the two stages rests on the insertion of a dry, compressionally heated, nonrotating, central downdraft of originally tropopause-level air in the transition to the more severe case. The quasisteady mature description of the thermohydrodynamic structure of each vortex is being developed, and then the conditions for transition from the moderately intense to the very intense vortex will be sought. The practical motivation is to make progress toward the highly desirable, but very formidable task of being able to anticipate which tropical storms or minimal hurricanes will evolve to supertyphoons.

With a description of the one-cell storm, believed adequate for present purposes, already available, description of the two-cell vortex is the current challenge. In particular, since the potential-vortex and surface-inflow subdivisions of the structure of a very intense vortex are in hand, a realistic picture of the updraft and its location are sought.

The modeling proceeds from basic thermohydrodynamic principles. Nonessential geometric detail, as well as association of conclusions with the details of particular parameterizations, is being avoided as much as possible.

Tentative results achieved thus far, by an integral-type treatment that seeks the location of the eye wall and its properties with height, point to a particularly sensitive dependence on the vertical variation of the angular momentum in the portion of the vortex outside the eye wall. Perhaps for only certain, narrowly defined stratifications of angular momentum may the conservation laws be compatible with two-cell structure for an intense atmospheric vortex.

## 1. INTRODUCTION

### 1.1 Statement of the Objective

The principal contribution still to be made in forecasting the intensity of tropical storms is to identify the observable(s) that permit one to anticipate (as much in advance as possible) which incipient storm will become hurricanes and which will not.<sup>#</sup>

Very roughly about half of all tropical storms, one-cell vortices extending vertically from sea level to tropopause and radially many hundreds of miles, transform into two-cell vortices (hurricanes) (Fendell 1974). The transition involves the insertion of a column of relatively dry, clear, nonrotating, tropopause-level air at the center of the vortex. Accordingly, the region of intensely swirling, very cloudy, torrentially raining updraft becomes an annulus surrounding that "eye" of dry air; i.e., an "eye" has then been inserted within an "eye wall". A formidable vortex, with a peak swirl of less than 100 mph and horizontal pressure deficit at sea level of roughly twenty millibars (the tropical storm, as defined here), can be transformed into a terrifying vortex with a peak swirl of some 200 mph and a pressure deficit of appreciably more than 50 mb (the hurricane, as defined here). An important question is: "what telltale observable, accessible to aircraft, satellites, etc., would permit one to anticipate the transition from tropical storm to hurricane?" The intensity of a tropical cyclone is not, of course, a simple monotonic increase with time to a peak, following by a simple monotonic decay; rather, there may be several transitions back and forth between one- and two-cell structure, suggestive of partial insertion, then removal, of an "eye" (Carrier 1971a).

---

<sup>#</sup>Gray (1979, p. 51) comments: "Tropical cyclone forecasters generally agree that skill at operational forecasting of tropical cyclone intensity change is nearly zero." He notes that trying to relate intensity to cloudiness configuration (as observed by passive satellites) is subject to significantly erroneous results, and furnishes inadequate detail. It may be noted that the gustiness of winds is not discussed, since treatment of the variance seems premature when prediction of the mean is still not possible. Gustiness factors for tropical cyclones (ratio of peak transient wind to wind sustained over a scale of one minute to five minutes, depending on the correlator) range from 1.0 to 1.8 in the literature (Brand et al 1979).

Normally, quantifying any details about structure in tropical cyclones is highly uncertain because proper formulation of turbulent diffusion, cumulus convection, and radiative transfer is unknown. These three important phenomena may well not have satisfactory representation in terms of macroscale variables, so the attempt at such parameterization incurs uncertainty. Yet such parameterization is entailed in virtually all contemporary tropical cyclone modeling.

## 1.2 An Approach to Two-Cell Structure for an Intense Atmosphere Vortex

Whereas most contemporary hurricane modeling entails direct numerical assault on all-inclusive mathematical formulation, here an alternative, approximate analytic treatment is utilized as much as possible (Carrier 1970; Carrier, Hammond and George 1971). The hurricane is subdivided logically into those parts in which different physical phenomena dominate; when a particular subdivision is treated, only that subset of the full equations that retains the locally dominant physical processes is solved. Such a subset is usually more tractable to solve, and parametric variation easier to examine. A composite global solution is synthesized from solutions to the subdomains by demanding appropriate continuity of dependent variables and their fluxes at interfaces.

Under the high-speed portion (only) of a severe rotating storm, the nonlinear "surface" inflow layer is inviscidly controlled; only in a very small sublayer (immediately contiguous to the ground) of the inflow layer does diffusion enforce the no-slip boundary condition (Carrier 1971b; Burggraf, Stewartson and Belcher 1971; Carrier and Fendell 1978). The diffusive sublayer becomes thinner, and the outer inflow layer thicker, as one moves toward the center of the vortex. [An analogous result is familiar in nonrotating contexts to aerodynamicists in the form of the following bit of well-known empiricism (e.g., Launder 1964): a near-wall diffusive layer becomes thinner in the direction of a favorable (i.e., accelerating) pressure gradient.] At sea level, the pressure is high at the lateral edge of the intense vortex and the pressure is greatly reduced at the center, such that a strong positive pressure gradient exists; thus, the low-level swirling flux (that erupts up the eye wall) is predominantly inviscidly controlled as it proceeds toward the hurricane center. The cited pressure gradient is radial, so the statement

of a limited role for frictional effects pertains primarily to the statement of conservation of radial momentum. However, the azimuthal-velocity profile is largely developed, such that further evolution of the surface-inflow-layer profile near the center of the vortex is not to be anticipated.

Radiative cooling is important only in the outer and less cloudy portions of the storm (Fendell 1974), and the simple well-defined model of moist-adiabatic ascent\* suffices to describe the locus of thermodynamic states in the eye wall. In the previous paragraph it is pointed out that the low-level flow entering the eye wall is nondiffusive. Two of the three processes that entail parameterization (specifically, turbulent diffusion and radiative transfer) do not enter significantly in the portion of the hurricane flow field critical to quantitative analysis of two-cell structure, and the third process (cumulus convection) can be formulated locally in a well-accepted, well-defined form.

The upshot is the following good fortune: one of the few questions about hurricane structure that can be definitively formulated by contemporary modeling happens to be one of the most important. Specifically, that question is, what is the balance of forces and thermodynamic states in the central region of a tropical storm that permits two-cell structure to arise as an alternative to one-cell structure?

### 1.3 The Boundary-Value Problem

For axisymmetric inviscid swirling flow in which a radial influx becomes an axial upflux, the boundary-value problem is well-defined. If one confines attention at the outset to low altitudes such that

---

\* Water-vapor-containing air rises, expands and cools dry-adiabatically (at constant water-vapor/air mixture ratio) until (in the absence of supercooling) the temperature drops far enough to imply saturation. Thenceforth, it continues to ascend such that saturation of water vapor is maintained at the local thermodynamic state, the condensed excess water substance falling out so that is unavailable for re-evaporative cooling. (Hence the process cannot be reversed.) The originally low-level, convectively unstable fluid undergoing this ascent is taken to rise too quickly to entrain any ambient air, and hence remains unmixed with cooler or drier air. In fact, of course, some mixing with nearby ambient air occurs and some re-evaporation into this unsaturated mix also occurs, but the no-mixing case is realistic enough to provide valuable insight.

incompressibility suffices, the formulation is available in texts (e.g., Batchelor 1967). Angular momentum is constant on streamlines, continuity is enforced, advective and centripetal accelerations balance the radial pressure gradient, and the total pressure head is constant across streamlines (Carrier, Dergarabedian and Fendell 1969). The annulus is bounded on one side by a free streamsurface that demarcates the eye wall interface with the eye, and on the other side by a free streamsurface that demarcates the eye wall interface with the outer vortex. The position of both these bounding streamsurfaces must be found in the course of solution, under enforcement of statements concerning the continuity of pressure. One result sought is the displacement of the eye wall from the axis of symmetry, which is also the axis of rotation. It is anticipated that this displacement ultimately increases with height.<sup>#</sup> The mathematically elliptic character of the boundary-value problem reflects the physical fact that streamwise and transverse derivatives, and streamwise and transverse velocity components, are of comparable magnitude; there is no single preferred direction of change.

Useful insight is attainable at the sacrifice of detail by using an "integral method" (Finlayson 1972), or one-dimensional approach. Roughly, one "forces" a parabolic-like character on the problem by effectively integrating out transverse dependence and then seeking streamwise variance from the simplified boundary-value problem.

---

<sup>#</sup>The increasing displacement of the eye wall from the axis with altitude seems likely under conservation of angular momentum, since density decreases with altitude. Conservation of mass also suggests that the cross-sectional area of the eye-wall annulus increases with altitude. The fact that the eye wall tilts radially outward with increasing height is suggested further by certain satellite photographs of hurricanes (Fendell 1974). If the eye wall were vertical, pressure deficits achievable under compressional heating in the eye could not serve as an explanation of intense swirl speeds observed in the eye wall (cf. Malkus and Riehl 1960).

## 2. A BOUNDARY-VALUE PROBLEM FOR THE TURNAROUND

An inviscid incompressible steady axisymmetric model of the turnaround region in a severe vortical storm is adopted, in cylindrical polar coordinates with origin at the ground on the axis of rotation (and of symmetry) (Figure 1).

The azimuthal, radial, and axial velocity components ( $v^*$ ,  $u^*$ , and  $w^*$ , respectively), in view of conservation of angular momentum and of conservation of mass, may be written [ $\Gamma^* = r_1^* V^*$ , where  $r_1^*$  is the (given) radius of peak swirl in region I, and where  $V^*$  is the (given) value of that peak swirl]

$$(r^*v^*)^2 = \Gamma^{*2}F(\psi) ; \quad (2.1)$$

$$-r^*u^* = \frac{\Gamma^*h^*}{\pi} \frac{\partial \psi}{\partial z^*} ; \quad (2.2)$$

$$r^*w^* = \frac{\Gamma^*h^*}{\pi} \frac{\partial \psi}{\partial r^*} . \quad (2.3)$$

Super asterisk denotes a dimensional quantity; no asterisk, a dimensionless quantity. The cylindrical radial coordinate is  $r^*$ ; the axial coordinate,  $z^*$ ; the maximum height of the surface inflow layer,  $h^*$ ; the streamfunction for the secondary flow (involving velocity components  $u^*$ ,  $w^*$ , only),  $\psi$ ; the function giving distribution of angular momentum with streamfunction,  $F$ .

Conservation of radial momentum is ( $\rho_d^*$  is density)

$$u^* \frac{\partial u^*}{\partial r^*} + w^* \frac{\partial u^*}{\partial z^*} + \frac{\partial}{\partial r^*} \left( \frac{p^*}{\rho_d^*} \right) = \frac{\Gamma^{*2}F(\psi)}{r^{*3}} . \quad (2.4)$$

Bernoulli's equation is

$$\frac{u^{*2} + w^{*2}}{2} + \frac{p^*}{\rho_d^*} + \frac{\Gamma^{*2}F(\psi)}{2r^{*2}} + g^*z^* = \frac{\Gamma^{*2}}{2r_1^{*2}} + \frac{p_1^*}{\rho_d^*} ; \quad (2.5)$$

in (2.5) the Bernoulli constant is taken as universal for all streamlines emerging from region II in view of the known relation

$$\frac{[u^*(r_1^*, z^*)]^2}{2} + \frac{\Gamma^{*2} F(\psi)}{2r_1^{*2}} = \frac{\Gamma^{*2}}{2r_1^{*2}} \quad (2.6)$$

and the fact that the pressure above hydrostatic is axially invariant for  $z^* \leq h^*$ , within the conventional boundary-layer approximation. Within the cyclostrophic approximation,

$$p_a^* - p_1^* \doteq (\rho_d^*/2)V^{*2} = (\rho_d^*/2)(\Gamma^{*2}/r_1^{*2}), \quad (2.7)$$

where  $p_a^*$  is the ground-level ambient pressure (given).

From a crude treatment of the turnaround, to be published elsewhere,  $(h^*/r_1^*) \doteq 0.2$  for relevant values of  $r_1^*$ ,  $V^*$ , where typical (given) values, for a severe tornado, are  $r_1^* \doteq 160$  m,  $V^* \doteq 100$  m/s.<sup>#</sup> In any case,  $h^*$  and  $r_1^*$  are taken as known. Thus, in addition to its use in (2.2) and (2.3),  $h^*$  is employed to nondimensionalize the independent variables:

$$x = \pi r^*/h^*, \quad y = \pi z^*/h^* . \quad (2.8)$$

Subtraction of the radial derivative of (2.5) from (2.4) gives

$$x \left( \frac{1}{x} \psi_x \right)_x + \psi_{yy} + \frac{F'(\psi)}{2} = 0 , \quad (2.9)$$

where subscripts  $x$  and  $y$  denote partial differentiation. The swirl profile  $F(\cdot)$  is known from conditions holding at  $x = x_1 = \pi r_1^*/h^* \equiv \pi/h$ . It is known from solution of region II (Carrier and Fendell 1978) that  $F$  is a monotonically increasing function of  $\psi$ , such that  $F(0) = 0$  and  $F(I) = 1$ , where the datum  $\psi(x > x_1, 0) = 0$  is adopted, and from (2.2) and (2.8),

<sup>#</sup>For a hurricane,  $(h^*/r_1^*) \doteq 0.1$ ,  $r_1^* \doteq 15$  km,  $V^* \doteq 100$  m/s.

$$\psi(x_1, \pi) = \int_0^{\pi} u(x_1, \zeta) d\zeta \equiv I, \quad (2.10)$$

where  $u = u^*/V^*$ , and, for completeness,  $v = v^*/V^*$ . Clearly, for  $F$  linear in  $\psi$ , (2.9) becomes Poisson's equation, and for  $F$  quadratic in  $\psi$ , (2.9) becomes Helmholtz's equation. Although, from known results for region II, such simple forms for  $F(\psi)$  are not detailed replications for  $(r^*v^*)/\Gamma^*$  of interest, still their tractability urges their adoption.

The pressure along the streamline that separates from  $y = 0$  at  $x = x_1$  remains at  $p_1^*$ , for the model of a nonrotating "eye" isobaric over an altitude range in which gravity implies negligible pressure changes. Then, from (2.5), since  $F(0) = 0$ ,

$$(\psi_x)^2 + (\psi_y)^2 = \left(\frac{x}{x_1}\right)^2 \quad \text{on } \psi = 0. \quad (2.11)$$

The pressure along the streamsurface  $\psi = I$ , which passes through the circle  $x = x_1$ ,  $y = r$ , should be consistent with the pressure in the potential-vortex region; hence

$$p(x, y) = p_1 + \left[1 - \left(\frac{x_1}{x}\right)^2\right], \quad (2.12)$$

from the cyclostrophic balance, where the nondimensionalization

$$p = \frac{p^*}{\frac{1}{2} \rho^* V^{*2}} \quad (2.13)$$

has been adopted. From (2.5), (2.12), and (2.13), with neglect of the gravitational term, since  $F(I) = 1$ ,

$$\psi_x^2 + \psi_y^2 = 0 \quad \text{on } \psi = I. \quad (2.14)$$

This condition merely states that there is no contribution from the secondary-flow velocity components  $u^*$ ,  $w^*$  to the pressure field, where region III interfaces with region I.

Equations (2.9), (2.11), and (2.14) constitute the boundary-value problem of interest, when supplemented by a relation for  $F(\psi)$ , obtained

from previously executed analysis of region II. By (2.1), (2.2), (2.6), and the fact that  $w(x_1, y) \doteq 0$ , the relation for  $F(\psi)$  gives implicitly an expression for  $\psi(x_1, y)$ ,  $0 \leq y \leq \pi$ , with which to initiate the analysis (see below). Finally, it is anticipated that  $\psi(x, y)$ , as given by the boundary-value problem is periodic in  $y$ ; this periodicity reflects the fact that the formulation must be revised after completion of about one cycle. More explicitly, it is anticipated that the locus of any streamline, say  $\psi = I/2$ , as  $y$  increases, decreases to a minimum value of  $x$ , then increases in  $x$  to recover its initial value  $x = x_1$  and to achieve a peak value in  $x$ , before decreasing back to  $x = x_1$  to begin another period. It is to be expected that the undulating flow so generated will be unstable somewhere along its trajectory, but the immediate goal is to find that flow and discussion of the stability problem is deferred until that is done. Of particular interest are the amount by which  $v$  exceeds the value associated with  $x = x_1$ ,  $\psi = I$ , and the values of  $x$  and  $\psi$  at which the maximum occurs.

For explicitness, a rough characterization of the function  $\psi(x_1, y)$ ,  $0 \leq y \leq \pi$ , is now presented. In the largely inviscid portion of region II, (2.6) may be rewritten as

$$u^2(x, y) + v^2(x, y) \doteq (x_1/x)^2. \quad (2.15)$$

From (2.1), (2.2), and (2.15), one obtains

$$-u(x_1, y) = \frac{\partial \psi(x_1, y)}{\partial y} = \left\{ 1 - [v(x_1, y)]^2 \right\}^{1/2} = [1 - F(\psi)]^{1/2}, \quad (2.16)$$

where  $0 \leq F(\psi) \leq 1$  for  $0 \leq \psi \leq I$ . Thus,  $\psi(x_1, y)$  is given by

$$y = \int_0^{\psi(x_1, y)} \frac{d\mu}{\left\{ 1 - [F(\mu)] \right\}^{1/2}} \quad (2.17)$$

where  $\psi \rightarrow I$  as  $y \rightarrow \pi$  [cf. (2.10)]. For  $F(\psi) = \psi/I$ ,

$$\psi = y \left( 1 - \frac{y}{2\pi} \right), \quad I = \frac{\pi}{2} \Rightarrow v^2(x_1, y) = \frac{2y}{\pi} \left( 1 - \frac{y}{2\pi} \right). \quad (2.18)$$

For  $F(\psi) = (\psi/I)^2$ ,

$$\psi = 2^{1/2} \sin(y/2), I = 2^{1/2} \Rightarrow v^2(x_1, y) = \sin^2(y/2). \quad (2.19)$$

In fact,

$$v(x_1, y) \doteq 1 - \exp\left(-\frac{c}{\pi} y\right), c \doteq 3, \quad (2.20)$$

might be more realistic, but is far less tractable.

In summary, if

$$\Psi(x, y) = \frac{\psi(x, y)}{I}, G'(\Psi) = \frac{F'(\psi)}{I}, \quad (2.21)$$

then the boundary-value problem is, for  $0 \leq \Psi \leq 1$ ,

$$x \left( \frac{1}{x} \Psi_x \right) + \Psi_{yy} + G'(\Psi) = 0; \quad (2.22)$$

$$\Psi_x^2 + \Psi_y^2 = \left( \frac{x}{Ix_1} \right)^2 \text{ on } \Psi = 0, \Psi_x^2 + \Psi_y^2 = 0 \text{ on } \Psi = 1; \quad (2.23a)$$

$$\Psi(x_1, y) \text{ given, with } \psi \text{ periodic in } y. \quad (2.23b)$$

One might consider interchanging the roles of the dependent variable  $\psi$  and the independent variable  $x$ , and using perhaps some technique within the framework of the method of weighted residuals to extract the desired information from (2.21)-(2.23). However, here alternative procedures are used to study (2.21)-(2.23).

### 3. TREATMENT OF A LOW-LEVEL SEPARATED LAYER WITHOUT STRUCTURE

The momentum balance in an axisymmetric separated boundary layer without structure is examined. The thin sheet (or "eye wall") is the demarcation between an "eye", isobaric at pressure  $p_1^*$ , and a potential vortex with radially dependent pressure given by (2.12). At  $r^* = r_1^*$ ,  $p^*$  in the sheet equals that in the "eye" (Figure 2).

Henceforth in this section the symbol  $r^*(z^*)$  denotes the outside surface of the "eye wall" without structure. At the point A, given by  $[r^*(z^*), z^*]$ , the principal radii of curvature are  $\{1 + [r^{*\prime}(z^*)]^2\}^{3/2}/r^{*\prime\prime}(z^*)$  and  $r^*(z^*)\{1 + [r^{*\prime}(z^*)]^2\}^{1/2}$ . Super prime denotes ordinary derivative with respect to the argument of the function. The velocity component in a plane containing the axis of symmetry is denoted  $q^*$ , while the velocity component (swirl) in a plane perpendicular to the axis of symmetry is denoted  $v^*$ . Thus, if  $\hat{t}$  is a unit vector in the plane containing the axis, and  $\hat{\theta}$  is perpendicular to  $\hat{t}$  and refers to the azimuthal component in a cylindrical-polar-coordinate system, then

$$\vec{v}^* = q^*\hat{t} = v^*\hat{\theta}. \quad (3.1)$$

The force balance perpendicular to the thin sheet at  $[r^*(z^*), z^*]$  equates the pressure gradient consistent with a potential vortex outside the sheet, to the component of acceleration perpendicular to the sheet. There are two contributions to the acceleration, each involving the square of a velocity component over an appropriate radius of curvature:

$$-\frac{\partial}{\partial h^*} \left( \frac{p^*}{\rho_d^*} \right) = \frac{q^{*2} r^{*\prime\prime}}{[1 + (r^{*\prime})^2]^{3/2}} - \frac{v^{*2}}{r^* [1 + (r^{*\prime})^2]^{1/2}}, \quad (3.2)$$

where  $h^*$  represents a coordinate running across the sheet.

Variations in velocity occurring across the sheet are not resolved ( $\Gamma^* \equiv r_1^* v^*$ ):

$$\int v^{*2} dh^* = \Gamma^{*2} \int \frac{dh^*}{[r^*(h^*)]^2} = r_1^{*2} v^{*2} \int \frac{dh^*}{[r^*(h^*)]^2} \equiv \frac{r_1^{*2} v^{*2} A^*}{r^{*2}} \Rightarrow$$

$$\frac{A^*}{r^{*2}} = \int \frac{dh^*}{[r^*(h^*)]^2} ; \quad (3.3)$$

$$\int q^{*2} dh^* = v^{*2} \int \left[ \frac{q^*(h^*)}{V^*} \right]^2 dh^* \equiv v^{*2} B^* \Rightarrow$$

$$B^* = \int \left[ \frac{q^*(h^*)}{V^*} \right]^2 dh^* . \quad (3.4)$$

The potential-vortex form of  $v^*$  is used in the definition of  $A^*$ .

From these definitions and from (2.12), to an accuracy that serves current purposes,

$$\frac{v^{*2}}{2} \left( 1 - \frac{r_1^{*2}}{r^{*2}} \right) = \frac{A^* v^{*2} r_1^{*2}}{r^{*3} [1 + (r^{*'})^2]^{1/2}} - \frac{B^* v^{*2} r^{*''}}{[1 + (r^{*'})^2]^{3/2}} . \quad (3.5)$$

The following nondimensionlization is introduced:

$$\bar{x} = \frac{r^*}{r_1^*} , \quad \bar{z} = \frac{z^*}{r_1^*} , \quad \alpha = \frac{2A^*}{r_1^*} , \quad \beta = \frac{2B^*}{r_1^*} . \quad (3.6)$$

If  $A^* = (h^*/2)$ ,  $B^* = (h^*/2)$ , seemingly reasonable values, then

$$\alpha \doteq \frac{h^*}{r_1^*} \equiv h , \quad \beta \doteq \frac{h^*}{r_1^*} \equiv h . \quad (3.7)$$

Under (3.6), (3.5) becomes ( $\alpha, \beta$  specified)

$$1 - \frac{1}{\bar{x}^2} = \frac{\alpha}{\bar{x}^3(1 + \bar{x}'^2)^{1/2}} - \frac{\beta \bar{x}''}{(1 + \bar{x}'^2)^{3/2}} \Rightarrow$$

$$\bar{x}'' = \frac{\alpha}{\beta} \frac{1 + \bar{x}'^2}{\bar{x}^3} - \frac{1}{\beta} \left( \frac{\bar{x}^2 - 1}{\bar{x}^2} \right) (1 + \bar{x}'^2)^{3/2}. \quad (3.8)$$

In this translationally invariant equation, it is taken that  $\bar{x}(\bar{z} = 0) = 1$ . It is shown below that  $\bar{x}$  is periodic in  $\bar{z}$ . Solution is sought for positive and negative  $\bar{z}$ , where the boundary conditions are

$$\bar{x}(0) = 1 \quad (3.9)$$

$$\bar{x}'(0) = \bar{x}'_0, \text{ given const. } > 0. \quad (3.10)$$

The boundary conditions preclude odd or even solution for  $\bar{x}$  and  $\bar{z}$ . Sought are  $\bar{x}^+$ , the largest value of  $\bar{x}$ , which occurs where  $\bar{x}' = 0$ , and  $\bar{x}^-$ , the smallest value of  $\bar{x}$ , which also occurs where  $\bar{x}' = 0$ . In that  $\bar{x}^- < 1$ , there is "overshoot" of the swirl, and, from (2.12), there is decrease of pressure from the value that holds in the "eye", i.e., in  $0 < r^* < r^*(z^*)$ ; it is reiterated that the magnitude of the swirl overshoot and pressure decrease are of particular interest.

While numerical integration of (3.8)-(3.10) is required ultimately, some preliminary treatment is helpful. Since (3.8) is translationally invariant in  $\bar{z}$ , phase-plane analysis is introduced (Figure 3):

$$\frac{d\bar{x}}{d\bar{z}} = \bar{p}(\bar{x}) \Rightarrow \frac{d^2\bar{x}}{d\bar{z}^2} = \frac{d\bar{p}(\bar{x})}{d\bar{z}} = \frac{d\bar{x}}{d\bar{z}} \frac{d\bar{p}}{d\bar{x}} = \bar{p} \frac{d\bar{p}}{d\bar{x}}. \quad (3.11)$$

Thus,

$$\frac{\beta \bar{p} \bar{p}'}{(1 + \bar{p}^2)^{3/2}} = \frac{\alpha}{\bar{x}^3(1 + \bar{p}^2)^{1/2}} + \frac{1}{\bar{x}^2} - 1. \quad (3.12)$$

The slope is infinite at  $\bar{p} = 0$  and is zero where

$$\frac{\alpha}{\bar{x}^3(1 + \bar{p}^2)^{1/2}} + \frac{1}{\bar{x}^2} - 1 = 0 ; \quad (3.13)$$

the intersection of the curve at (3.13) with the  $\bar{p} = 0$  ray is given by

$$\frac{\alpha}{\bar{x}_*^3} + \frac{1}{\bar{x}_*^2} - 1 = 0 , \quad (3.14)$$

where  $\bar{x}_* = 1$  for  $\alpha = 0$ ,  $\bar{x}_* > 1$  for  $\alpha > 0$ . For  $1 \gg \alpha > 0$ ,  
 $\bar{x}_* = 1 + (\alpha/2) - (3\alpha^2/8) + \dots$

Although the following development is not pursued to the extent of obtaining results, it may be worth noting that if

$$H(\bar{x}) = (1 + \bar{p}^2)^{-1/2} , \quad (3.15)$$

then (3.12) becomes

$$-BH' = \frac{\alpha H}{\bar{x}^3} + \frac{1}{\bar{x}^2} - 1. \quad (3.16)$$

If

$$\tau = \bar{x}^{-2} , \quad (3.17)$$

then

$$2\beta \frac{dH}{d\tau} - \alpha H = \tau^{-1/2} - \tau^{-3/2} , \quad (3.18)$$

or

$$H = (\beta\tau^{1/2})^{-1} - \left(\frac{\pi}{2\alpha\beta}\right)^{1/2} \left(1 + \frac{\alpha}{\beta}\right) \exp\left(\frac{\alpha\tau}{2\beta}\right) \operatorname{erfc}\left(\frac{\alpha\tau}{2\beta}\right)^{1/2} + E \exp\left(\frac{\alpha\tau}{2\beta}\right) , \quad (3.19)$$

where E is a const. of integration. From (3.15), (3.17), and the definition  $\bar{p} \equiv (d\bar{x}/d\bar{z})$ , one may write formally

$$\frac{d\bar{x}}{d\bar{z}} = \left\{ 1 + [H(\tau)]^{-2} \right\}^{1/2} = \frac{d(\tau^{-1/2})}{d\bar{z}}. \quad (3.20)$$

Thus,

$$d\bar{z} = \frac{d(\tau^{-1/2})}{\left\{ 1 + [H(\tau)]^{-2} \right\}^{1/2}}, \quad (3.21)$$

where  $H(\tau)$  is given by (3.19).

For the special case  $\alpha = 0$ , i.e., no swirl, multiplication of (3.12) by  $\bar{x}'$  yields

$$\frac{\beta}{(1 + \bar{x}'^2)^{1/2}} = \frac{(\bar{x} - 1)^2}{\bar{x}} + \frac{\beta}{m}, \quad (3.22)$$

where the constant of integration has been written as  $(\beta/m)$ , with

$$m \equiv (1 + \bar{x}_0'^2)^{1/2} \quad (3.23)$$

for consistency. It is recalled that  $\bar{x}_0' (\equiv d\bar{x}(0)/d\bar{z})$  is a given positive finite constant. Inspection of (3.22) reveals that  $\bar{x}'$  is maximum at  $\bar{x} = 1$ , so  $(1 + \bar{x}_0'^2)^{1/2}$  is the maximum value of  $(1 + \bar{x}'^2)^{1/2}$ , whence the symbol  $m$ . At  $\bar{x}' = 0$ ,

$$\bar{x}^{\pm} = 1 + \frac{\beta}{2} \left( 1 - \frac{1}{m} \right) \pm \left[ \frac{\beta}{2} \left( 1 - \frac{1}{m} \right) \right]^{1/2} \left[ 2 + \frac{\beta}{2} \left( 1 - \frac{1}{m} \right) \right]^{1/2}. \quad (3.24)$$

For  $\bar{x}_0' \rightarrow 0$  so  $m \rightarrow 1$ ,  $\bar{x}^{\pm}$  merge to unity; this case involves a vertically separating surface inflow layer, and hence no overshoot. For  $\bar{x}_0' \rightarrow \infty$  so  $m \rightarrow \infty$ ,  $\bar{x}^{\pm}$  remain bounded:

$$\bar{x}^{\pm} = 1 + \frac{\beta}{2} \pm \left( \frac{\beta}{2} \right)^{1/2} \left[ 2 + \frac{\beta}{2} \right]^{1/2}; \quad (3.25)$$

this case involves effectively horizontal inflow of the separating surface inflow layer, and leads to the minimum value of  $\bar{x}^-$  for fixed  $\beta$ . For  $\beta = 0.1$ ,  $\bar{x}^+ \doteq 1.37$  and  $\bar{x}^- \doteq 0.73$ ; for  $\beta = 0.2$ ,  $\bar{x}^+ \doteq 1.56$  and  $\bar{x}^- \doteq 0.64$ .

The plausible range of  $\beta = 0(0.2)$ , from a crude analysis of the turnaround to be published separately; it is recalled that  $\beta$  is associated with in-plane motion. These results suggest what proves to be a general trend:  $\bar{x}^-$  decreases as  $\bar{x}'_0$  and  $\beta$  increase.

Finite values for  $\alpha$  indicate finite swirl; increasing  $\alpha$  yields larger  $\bar{x}^-$  and smaller overshoot. From results of numerical integration, for finite  $\alpha$ ,  $\bar{x}^\pm$  approach finite values as  $\bar{x}'_0 \rightarrow \infty$  for fixed  $\beta$ . For the plausible values  $\alpha = \beta = 0.2$ , for  $\bar{x}'_0 = 2, 5, 10$ , the corresponding values of  $\bar{x}^- = 0.77, 0.72, 0.70$ . Hence, swirl overshoots in the range of about 20% seems plausible, but not much more; estimates that swirl in the turnaround exceeds the swirl at  $\bar{x} = 1, \bar{z} = h$  [in terms of the definitions of (3.6)] by about 100% (Lewellen 1977) are excessive according to this analysis. Further results are given in Table 1 and graphical presentation is given in Figures 4 and 5.

As suggested earlier, the periodic nature of the mathematical solution is not observed physically; rather "vortex breakdown" (Hall 1972; Leibovich 1978) intervenes, and no attempt is undertaken here to describe, via the *inviscid model developed in this section*, details of the breakdown process. Rather, the following inferences are drawn concerning two-cell vortical structure. An inviscid theory suffices to describe the nearly horizontal separation of the bulk of the low-level inflow layer, which turns upward (with a maximum local swirl speed probably not much more than 20% greater than the peak outer-vortex value), undergoes a breakdown, and emerges as a vertical free layer. The further evolution with altitude of the layer is treated in the next section by a model which retains buoyancy, density variation, and change of angular momentum with height; that model is intended to hold through a considerable depth of the troposphere, if not all the way to the tropopause.

The relatively thin, diffusive, very-low-level subregion of the inflow layer may possibly continue inward to the axis and fill the very bottom of the central region, if the compressionally heated downflux in the eye does not extend from tropopause all the way to surface level. This "filling flow" emanating from thin diffusive inflow sublayer may be plausibly pictured as a flux that at greater height serves as a transition between (1) the modest recirculatory motion in the relatively dry

and nonrotating eye, and (2) the relatively rapidly rotating and ascending air of the eye wall, which is characterized by a near-moist-adiabatic locus of thermodynamic states. Indeed, the mass and momentum interchange owing to the shearing interaction along the fairly well-defined free boundary between the eye and the eye wall constitutes a possibly fruitful line of future inquiry concerning core structure in a mature severe vortex. The entrainment process between a fast-moving stream and an adjacent, nearly stagnant stream is not fully understood, and existence of a significant swirling component of velocity in the high-speed stream only further complicates the subject. This matter is taken up again later when suggestions about future directions of investigation are set forth, but the above preliminary comments at this point seem apropos.

#### 4. A ONE-LAYER TREATMENT OF THE EYE WALL

While some repetition is inevitably entailed, a self-contained derivation of a one-layer treatment of the eye wall that holds through the depth of the troposphere is now given. It is useful as a start to review some tenets of the overall model of the mature vortical storm.

The general character of the configuration is given in Figure 6. In region I any radial and/or vertical motion is supposed to be so small that it is ignorable in the dynamic balance. The angular momentum  $\Gamma^*$  is prescribed, most simply as a constant, but probably more pertinently as a function of altitude  $z^*$ . The ambient thermodynamic state holding at each  $z^*$  at  $r_0^*$  is taken as known. Region II is the boundary layer in which swirling fluid moves radially inward;  $r_1^*$  is the radius near ground level at which the pressure in the potential vortex of region I is the same as the pressure at  $r^* = 0, z^* = 0$  when a fully developed eye extends from the tropopause altitude  $z_t^*$  to  $z^* = 0$ . Region III contains swirling, updraft fluid and its state trajectory is dynamically moist adiabatic; i.e., the total enthalpy (based on sea-level ambient conditions) is constant. Region IV is nearly stagnant and contains recompressed air from  $z_t^*$ , the altitude at which, in the ambient, the total enthalpy is the same as that at surface level. Typically, that ambient enthalpy has a profile with altitude of the character depicted in Figure 7. Recompressed air from  $z_t^*$  may not entirely fill region IV for cases in which the insertion of an eye is incomplete; the lower portion of region IV is then characterized by moist-adiabatic air, and the pressure at  $r^* = 0, z^* = 0$  is higher than that holding for a completely developed eye. The locus of thermodynamic states characterizing the portion of region IV filled with recompressed air is dry-adiabatic, with the (moisture-free) state at  $z_t^*$  serving as a reference; the thermodynamic state holding for the lower portion (if any) of region IV not filled with recompressed tropopause-level air is obtained from hydrostatics and the pressure-density pairings for the previously discussed moist adiabat, the pressure and altitude (but not the density) being continuous at the interface between dry-adiabatic air and moist-adiabatic air. It has already been noted in previous sections that the site of region III must be found in the course of solution.

Finding the locus of thermodynamic states that characterizes the moist adiabat based on sea-level ambient conditions, assigning an altitude to the tropopause  $z_t^*$ , and determining the pressure distribution with height in region IV, denoted  $p_{eye}^*(z^*)$ , are standard steps (Fendell 1974). However, some remarks about the moist adiabat are presented in Appendix A.

In a generalization of previous notation, the pressure in region I is denoted  $p_1(r^*, z^*)$ , where  $p_1(r_0^*, z^*) \equiv p_{amb}^*(z^*)$ , given, where "amb" abbreviates "ambient" and the two subscripts are used interchangeably. In conventional notation, if the subscript unity is discarded for the moment for brevity, in region I,

$$\frac{p^*}{r^*} \doteq \rho^* v^{*2}/r^* , \quad (4.1)$$

$$-\frac{p^*}{z^*} \doteq \rho^* g^* ; \quad (4.2)$$

hence,

$$g^* \frac{p^*}{r^*} = - \frac{v^{*2}}{r^*} \frac{p^*}{z^*} = - \frac{\Gamma^{*2}(z^*)}{r^{*3}} \frac{p^*}{z^*} . \quad (4.3)$$

If one seeks solution in the form

$$p^*(\eta^*) = p^*[m^*(z^*) - s^*(r^*)] , \quad (4.4)$$

one obtains (if prime denotes the ordinary derivative)

$$p^{*'}(\eta^*) [g^* s^{*'}(r^*) r^{*3} - \Gamma^{*2}(z^*) m^{*'}(z^*)] = 0 ; \quad (4.5)$$

i.e., without loss of generality,

$$s^*(r^*) = - \frac{1}{2g^* r^{*2}} , \quad (4.6)$$

$$m^*(z^*) = \int^{z^*} \frac{dz'}{\Gamma^{*2}(z')} . \quad (4.7)$$

For the special case of a vortex in region I that is invariant with altitude,  $\Gamma^* = \Gamma_0^*$ , const.,

$$m^*(z^*) = z^*/\Gamma_0^{*2}; \quad (4.8)$$

the choice of  $p^*(\eta^*)$  which matches the ambient atmosphere at  $r^{*-2} \ll 1$  is (restoring the subscript unity)

$$p_1^* = p_{\text{ambient}}^* \left[ z^* + \Gamma_0^{*2}/(2g^*r^{*2}) \right]. \quad (4.9)$$

[In this approximation the ambient formally is taken to hold at an infinite radial distance, but the discrepancy from a match to an ambient at a value of  $(r_0^*/r_1^*)$  of only ten results in an error of about merely one percent.]

For the somewhat more plausible case of a vortex, the angular momentum of which decreases linearly from a value of  $\Gamma_0^*$  at sea-level to zero at the tropopause  $z^* = z_t^*$ ,

$$\eta^* = \frac{z_t^*}{z_t^* - z^*} + \frac{\Gamma_0^{*2}}{2g^*r^{*2}z_t^*}, \quad (4.10)$$

such that at  $r^* \rightarrow \infty$ ,

$$z^* = \frac{z_t^*(\eta^* - 1)}{\eta^*}. \quad (4.11)$$

Thus a solution of the first-order partial differential equation  $p^*(\eta^*)$ , any function of  $\eta^*$ , also satisfies the boundary condition,

$$p_1^*(\eta^*) \rightarrow p_{\text{ambient}}^*(z^*) \text{ for } r^* \rightarrow \infty,$$

if one takes as the function

$$p_1^*(\eta^*) = p_{\text{ambient}}^* \left[ \frac{z^* + \frac{\Gamma_0^{*2}(Mz_t^* - z^*)}{2g^*r^{*2}Mz_t^*}}{1 + \frac{\Gamma_0^{*2}(Mz_t^* - z^*)}{2g^*r^{*2}Mz_t^{*2}}} \right]. \quad (4.12)$$

Here  $M$  is an assignable parameter in the range  $\infty < M \leq 1$ . Larger values of  $M$  reduce the effective dependence of the angular momentum on  $z^*$  and, indeed, as  $M \rightarrow \infty$  this equation degenerates to equation (4.9).

More generally, if  $\Gamma^*(z^*) = \Gamma_0^* [(z_t^* - z^*)/z_t^*]^n$ , then

$$p_1^*(\eta^*) = \begin{cases} p_{amb}^* \left\{ z_t^* - (z_t^* - z^*) \left[ 1 - \frac{(1-2n)}{(z_t^* - z^*)^{1-2n}} \frac{\Gamma_0^{*2}}{2g^*r^{*2}z_t^{*2n}} \right]^{\frac{1}{1-2n}} \right\}, & n \neq \frac{1}{2} \\ p_{amb}^* \left\{ z_t^* - (z_t^* - z^*) \exp \left[ -\Gamma_0^{*2}/(2g^*r^{*2}z_t^*) \right] \right\}, & n = \frac{1}{2}. \end{cases} \quad (4.13)$$

Finally, if  $\Gamma^*(z^*) = \Gamma_0^* \exp(-a^*z^*)$ , then

$$p_1^*(\eta^*) = p_{amb}^* \left\{ z^* + (2a^*)^{-1} \ln \left[ 1 + \frac{\Gamma_0^{*2} a^*}{g^*r^{*2} \exp(2a^*z^*)} \right] \right\}. \quad (4.14)$$

Thus, the deviation of the isobars from their asymptotic form as horizontal planes, owing to rotation, is known throughout region I for several stratifications of the angular momentum. This deviation is of significance in ascertaining the pressure differential at any altitude between the edge of the eye wall contiguous to the vortex of region I and the edge of the eye wall contiguous to the eye of region IV, where the eye wall is envisioned as a relatively narrow layer. More explicitly, in region III the pressure on the streamline contiguous to region IV must match the specified  $p_{eye}^*(z^*)$  in the eye, and the pressure on the streamline contiguous to region I must match the pressure in the potential vortex  $p_{ambient}^* \left[ m^{*-1} (m^*(z^*) - s^*(r^*)) \right]$ . These statements constitute the boundary conditions for the eye-wall calculation, to which attention is now turned.

The symbol  $R^*(z^*)$  henceforth denotes the radial displacement of the outside surface of the "eye wall" with structure; the symbol  $h^*(z^*)$  denotes the transverse thickness of the eye wall, though the eye wall is taken as thin, so  $h^*(z^*) \ll R^*(z^*)$ . The velocity component in a plane containing the axis of symmetry continues to be denoted by  $q^*$ , while the velocity component in a plane perpendicular to the axis of symmetry

continues to be denoted  $v^*$ . The angular momentum, in general  $r^*v^*(r^*,z^*)$ , is denoted  $\Gamma^*(z^*)$ ; at  $r^* = r_0^*$ , the outer edge of the vortex, the static pressure  $p_1^*(r^*,z^*) \rightarrow p_1^*(r_0^*,z^*) \equiv p_{amb}^*(z^*)$ , a measured quantity, where  $r_0^* \gg R^*(z^*)$ . The pressure at the interface between the eye wall and the inviscid vortex of region I is given by  $p_1^*[R^*(z^*),z^*] = p_{amb}^* \left\{ m^{*-1} [m^*(z^*) - s^*(R^*(z^*))] \right\}$ , where the formulae for  $m^*(z^*)$  and  $\Gamma^*(z^*)$  are given above. The pressure at the interface between the eye and the eye wall is given by  $p_{eye}^*(z^*)$ . The symbol  $z_*^*$  denotes the altitude down to which hydrostatic, adiabatic compression (of air whose with reference thermodynamic state is that of the ambient at  $z_t^*$ ) defines  $p_{eye}^*(z^*)$ , where, again,  $z_t^*$  is the altitude of the tropopause (the altitude at which the pressure and temperature of the ambient match that of ground-level air which has passed through the locus of thermodynamic states referred to as the moist adiabat). For  $z_*^* \geq z^* \geq 0$ ,  $p_{eye}^*(z^*)$  is defined by hydrostatics, and by moist-adiabatic states such that the pressure is continuous at  $z^* = z_*^*$ . If  $z_*^* = 0$ , then, in  $R^*(z^*) > r^* \geq 0$ , the dry-adiabatic relation holds through the entire depth of the troposphere, defined here as  $z_t^* \geq z^* \geq 0$ .

It is perhaps also worth reiterating that standard thermohydrostatic calculation gives  $p_{eye}^*(z^*)$  and  $z_t^*$  from specification of  $p_{amb}^*(z^*)$ ; in the course of such a calculation the triplet  $(\rho_{moist}^*, T_{moist}^*, p_{moist}^*)$  has been associated, where  $p_{moist}^*$  ranges between  $p_{amb}^*(0)$  and  $p_{amb}^*(z_t^*)$ , and the subscript moist designates moist-adiabatic [defined as the dry adiabatic, with constant water-vapor/dry-air mixing ratio, until saturation and as the conventional pseudo-adiabat above saturation (see Appendix A)].

It is convenient to introduce the concept of a series of calculations,  $i = 1,2,3\dots$  for known  $p_{amb}^*(z^*)$ ,  $T_{amb}^*(z^*)$ ,  $\rho_{amb}^*(z^*)$  and given  $\Gamma^*(z^*)$ . These calculations are based on different completeness of "flushing" of moist-adiabatic air from the eye as denoted by  $z_*^{*(i)}$ ,  $i = 1,2,3\dots$ . For example, one could study

$$z_*^{*(i)} = \frac{i-1}{N} z_t^*, \quad i = 1,2,3,\dots, N+1, \quad (4.15)$$

where  $i = 1$  would constitute an eye fully flushed of moist air, i.e., a completely developed dry-adiabatic eye, and  $i = N + 1$  would constitute a

degenerate case of no flushing, i.e., no insertion of dry-adiabatic air in the core. It may be anticipated that the theory advanced here is limited to cases in which  $z_*^*$  is a large fraction of  $z_t^*$ ; i.e., attention is at the outset confined to fully, or near fully developed, eyes.

It is perhaps also worth a brief digression to point out explicitly that the use of hydrostatics constitutes a limitation on what the present approach can ascertain about eye insertion, which in its early stages may well require retention of dynamical considerations. A fruitful direction may be modification of conventional plume theory, which yields the vertical profiles of transversely averaged quantities for buoyant axisymmetric columns over maintained low-level mass, momentum, and heat sources. The modification would entail generalization to spin-up in swirling environments, since the conventional theory is for steady plumes in a nonrotating environment; what efforts exist for swirling environments do not undertake temporal evolution of spin-up. The modification would also entail inclusion of provision for a downdraft core enveloped by an updraft annulus, since conventional plume theory is for so-called one-celled structure only (updraft everywhere).

It is useful to introduce the peak swirl speed of a potential vortex (with a nonrotating core) supportable by the surface-level pressure deficit between eye and ambient, under the cyclostrophic approximation:

$$p_{amb}^*(0) - p_{eye}^{(i)}(0) \doteq \frac{1}{2} \rho_{amb}^*(0) [v^{*(i)}]^2, \quad (4.16)$$

where taking the density fixed at its ambient value is adequate for present purposes, and the superscript  $i$  is recalled to denote the completeness of eye flushing. For  $i = 1$ , the swirl speed is maximum, and this value is used for nondimensionalization below.

The reference value for the angular momentum  $\Gamma_0^*$  is taken to be

$$\Gamma_0^* = r_1^* v^{*(1)}, \quad (4.17)$$

where  $r_1^*$  is the (specified) radius at which the surface inflow layer separates. If  $\Gamma_0^*$  is held fixed for all  $i$ , then, if

$$r_0^{*(i)} v^{*(i)} \equiv \Gamma_0^* \Rightarrow r_0^{*(i)} = \Gamma_0^* / v^{*(i)}, \quad (4.18)$$

it follows that

$$r_0^{*(1)} = r_1^*; r_0^{*(i)} > r_0^{*(i-1)}, \text{ since } v^{*(1)} > v^{*(i)}, i > 1. \quad (4.19)$$

Also, reference values for the streamwise and swirl components of velocity in the eye wall are taken as follows:

$$q_0^{*(i)} = (0.7)v^{*(i)}, v_0^{*(i)} = (0.5)v^{*(i)}. \quad (4.20)$$

It may be noted that

$$\left[ q_0^{*(i)} \right]^2 + \left[ v_0^{*(i)} \right]^2 \neq \left[ v^{*(i)} \right]^2; \quad (4.21)$$

while such an equality holds in the inviscid portion of the surface inflow layer and hence in the low-level turn-around, no such equality is appropriate for the eye wall after the losses associated with the breakdown. The factors (0.7) and (0.5) are rough intuitive guesses, and better insight is not anticipated to be available in the near future.

By conservation of angular momentum for the eye wall,

$$\left[ R^{*(i)}(z^*) \right] \left[ v^{*(i)}(z^*) \right] = r_0^{*(i)} v_0^{*(i)}. \quad (4.22)$$

As noted earlier, nondimensionalization is taken as follows:

$$R^{(i)}(z) \equiv \frac{R^{*(i)}(z^*)}{r_0^{*(1)}}, v^{(i)}(z) = \frac{v^{*(i)}(z^*)}{v^{*(1)}}, z = \frac{z^*}{r_0^{*(1)}}. \quad (4.23)$$

$$\left[ R^{(i)}(z) \right] \left[ v^{(i)}(z) \right] = \Sigma_1^{(i)}, \text{ where } \Sigma_1^{(i)} = \frac{r_0^{*(i)} v_0^{*(i)}}{r_0^{*(1)} v^{*(1)}} = 0.5. \quad (4.24)$$

By conservation of mass for the eye wall,

$$\left[ \rho_{\text{moist}}^*(z^*) \right] \left[ q^{*(i)}(z^*) \right] \left[ R^{*(i)}(z^*) \right] \left[ h^{*(i)}(z^*) \right] = \rho_{\text{eye}}^{*(i)}(0) q_0^{*(i)} r_0^{*(i)} h_0^{*(i)}, \quad (4.25)$$

where, for a thin layer, it is reasonable to adopt

$$h_0^{*(i)} = \kappa r_0^*, \text{ given,}$$

where  $r_0^* = 300\text{-}500$  miles for a hurricane,  $r_0^* = 6\text{-}8$  miles for a tornado, and  $\kappa = 0.0025$  for both. If one defines

$$\rho_{\text{moist}}(z) \equiv \frac{\rho_{\text{moist}}^*(z^*)}{\rho_{\text{eye}}^{*(1)}(0)}, \quad q^{(i)}(z) \equiv \frac{q^{*(i)}(z^*)}{v^{*(1)}}, \quad h^{(i)}(z) = \frac{h^{*(i)}(z^*)}{r_0^{*(1)}}, \quad (4.26)$$

then

$$\left[ \rho_{\text{moist}}(z) \right] \left[ q^{(i)}(z) \right] \left[ R^{(i)}(z) \right] \left[ h^{(i)}(z) \right] = \Sigma_2^{(i)}, \quad (4.27)$$

where

$$\begin{aligned} \Sigma_2^{(i)} &\equiv (0.7) \frac{\rho_{\text{eye}}^{*(i)}(0)}{\rho_{\text{eye}}^{*(1)}(0)} \frac{v^{*(i)}}{v^{*(1)}} \frac{r_0^{*(i)}}{r_0^{*(1)}} \frac{\kappa r_0^*}{r_0^{*(1)}} \\ &= (0.7)\kappa \frac{\rho_{\text{eye}}^{(i)}(0)}{\rho_{\text{eye}}^{(1)}(0)} \frac{r_0^*}{r_0^{*(1)}}. \end{aligned} \quad (4.28)$$

Since there is taken to be a constant head across all streamlines of the eye wall, Bernoulli's equation, generalized from the form employed earlier for the turnaround by the inclusion of density variation (where the moist-adiabatic locus relating pressure and density is recalled to be appropriate for the eye wall) and of gravitational effects, is ( $g^*$  is the magnitude of the gravitational acceleration)

$$\frac{[q^{*(i)}]^2 + [v^{*(i)}]^2}{2} + g^* z^* + \int_{p_{ref}^{*(i)}}^{p^{*(i)}} \frac{dp_1^*}{\rho_{moist}^*(p_1^*)} = \frac{[q_0^{*(i)}]^2 + [v_0^{*(i)}]^2}{2} \quad (4.29)$$

If one defines

$$p^{(i)}(z) = \frac{p^{*(i)}(z^*)}{p_{eye}^{*(1)}(0)}, \quad (4.30)$$

where

$$p^{*(i)}(z^*) = \frac{1}{2} \left\{ p_{amb}^* \left\{ m^{*-1} [m^*(z^*) - s^* (R^{*(i)}(z^*))] \right\} + p_{eye}^{*(i)}(z^*) \right\}, \quad (4.31)$$

and

$$p_{ref}^* = p^{*(i)}(0), \quad (4.32)$$

then

$$\left[ q^{(i)}(z) \right]^2 + \left[ v^{(i)}(z) \right]^2 + \Sigma_3 z + \Sigma_4 \int_{p_{ref}}^{p^{(i)}(z)} \frac{dp_1}{\rho_{moist}(p_1)} = \Sigma_5^{(i)} \quad (4.33)$$

where

$$\Sigma_3 \equiv \frac{2g^* r_0^{*(1)}}{[v^{*(1)}]^2}, \quad \Sigma_4 \equiv \frac{p_{eye}^{*(1)}(0) / \rho_{eye}^{*(1)}(0)}{[v^{*(1)}]^2 / 2},$$

$$\Sigma_5^{(i)} \equiv \left[ (0.7)^2 + (0.5)^2 \right] \left[ \frac{v^{*(i)}}{v^{*(1)}} \right]^2. \quad (4.34)$$

While the dimensionless form of the Bernoulli equation just derived is the form useful in the computations described below, it seems worthwhile to note implication derived by differentiation of the dimensional

form of the equation with respect to  $z^*$ ; if

$$\left[ \tau^{*(i)}(z^*) \right]^2 \equiv \left[ q^{*(i)}(z^*) \right]^2 + \left[ v^{*(i)}(z^*) \right]^2, \quad (4.35)$$

then,

$$\rho_{z^*}^{*(i)} + \frac{\rho_{\text{moist}}^*}{2} \left[ \tau^{*(i)} \right]^2 + \rho_{\text{moist}}^* g^* = 0. \quad (4.36)$$

But by definition,

$$\rho^{*(i)} = \frac{1}{2} \left( \rho_{\text{eye}}^{*(i)} + \rho_{\text{amb}}^* \right), \quad (4.37)$$

so that by use of hydrostatics,

$$\rho_{z^*}^{*(i)} = \frac{1}{2} \left( \rho_{\text{eye } z^*}^{*(i)} + \rho_{\text{amb } z^*}^* \right) = - \frac{1}{2} \left( \rho_{\text{eye}}^{*(i)} + \rho_{\text{amb}}^* \right) g^*. \quad (4.38)$$

Thus,

$$\left[ \tau^{*(i)} \right]_{z^*}^2 = \left( \frac{\rho_{\text{eye}}^{*(i)} + \rho_{\text{amb}}^* - 2\rho_{\text{moist}}^*}{\rho_{\text{moist}}^*} \right) g^*. \quad (4.39)$$

In general, for fixed  $z^*$ ,  $\rho_{\text{amb}}^* > \rho_{\text{moist}}^* > \rho_{\text{eye}}^*$ ; whereas  $\rho_{\text{amb}}^*$  appreciably exceeds  $\rho_{\text{moist}}^*$  probably only for tornado-prone ambients (e.g., cold air overriding moist air in the American Midwest),  $\rho_{\text{moist}}^*$  appreciably exceeds  $\rho_{\text{eye}}^*$  except for a fairly deep base of moist-adiabatic air in the very near-axis region of the vortex (e.g., hurricanes, which in fact usually do not have fully dry, fully developed eyes). The point is that the factor  $(\rho_{\text{eye}}^{*(i)} + \rho_{\text{amb}}^* - 2\rho_{\text{moist}}^*)$  may be negative, such that the two-cell structure being outlined may prove compatible with only certain ambient stratifications; for if the just-cited factor is negative,  $\left[ \tau^{*(i)} \right]^2$  itself may turn negative, i.e., the postulated two-cell structure cannot be realized. Thus, the relation for  $\left[ \tau^{*(i)} \right]_{z^*}^2$  not only furnishes a means of checking numerical accuracy, but also provides a hint that the present development may be able to distinguish between circumstances compatible with two-cell structure and circumstances incompatible with such structure.

Finally, the balance of the pressure gradient across the eye-wall layer with accelerations in the layer yields an equation that is a slight generalization of one given earlier for the turnaround:

$$\Sigma_4 \frac{p_{amb}^{(i)}(z; R^{(i)}) - p_{eye}^{(i)}(z)}{[\rho_{moist}^{(i)}(z)] [h^{(i)}(z)]} = \frac{[v^{(i)}(z)]^2}{R^{(i)} [1 + (R_z^{(i)})^2]^{1/2}} - \frac{[q^{(i)}(z)]^2 R_{zz}^{(i)}}{[1 + (R_z^{(i)})^2]^{3/2}} \quad (4.40)$$

Conservation of angular momentum, conservation of mass, Bernoulli's equation, and the balance of forces just stated constitute four equations for the four dependent variables  $R^{(i)}(z)$ ,  $v^{(i)}(z)$ ,  $q^{(i)}(z)$ , and  $h^{(i)}(z)$ . Four dimensionless parameters must be specified:  $\Sigma_2^{(i)}$ ,  $\Sigma_3$ ,  $\Sigma_4$ , and  $\Sigma_5^{(i)}$ ; further, the stratification of a storm-prone (convectively unstable) ambient, e.g., relative humidity and temperature as a function of pressure through the depth of the troposphere, must be specified, so that thermo-hydrostatic calculations giving  $z_t$ ,  $p_{eye}(z)$ ,  $\rho_{moist}(z)$  as a function of  $p_{moist}(z)$  [later identified with  $\frac{1}{2}(p_{eye} + p_{amb})$ ], etc., may be carried out. Aside from universal constants such as  $g^*$ , specification of the four above-cited dimensionless parameters actually entails specification of the reference thickness of the inflow layer,  $\kappa r_0^*$ ; the radial distance from the axis at which the surface inflow layer separates,  $r_1^*$ ; the height to which moist-adiabatic air remains in the core,  $z_*^{(i)}$ ; the variation of the angular momentum of the inviscid vortex  $\Gamma^*$  with height,  $z^*$ , where  $\Gamma^* = \Gamma_0^*$  at the surface  $z^* = 0$ , and, to reiterate,  $\Gamma_0^* = r_1^* v_*^{(1)}$ ,  $v_*^{(1)}$  being the near-surface peak swirl speed of a potential vortex with a non-rotating core ( $r_1^* > r^* > 0$ ) and a fully developed eye, for a given ambient thermodynamic state.

The set (4.24), (4.27)-(4.28), (4.33)-(4.34), and (4.40) can be reduced, by substitution of the first three into the last, to one second-order nonlinear ordinary differential equation for  $R(z)$ ; admittedly, the factor  $q(z)$  is expressed in terms of an intricate functional of  $R(z)$ , but the reduction is still convenient for numerical integration on a high-speed digital computer. Such integration requires identification of two boundary conditions; these are taken to be (for a vertically rising eye wall after breakdown, taken to occur at so low an altitude that  $z \doteq 0$ )

$$R_z(0) = 0, R(0) \text{ chosen such that } R_{zz}(0) = 0 \text{ in (4.40).} \quad (4.41)$$

Conceptually, this initial-value problem may then be marched forward in  $z$  from  $z = 0$  to  $z = z_t$  (or even further if extrapolation of tabulated data is accepted). In practice, singular behavior virtually always intervenes, such that some physical condition of the formulation is violated, and further calculation is not justified. For example, the layer is taken thin, but if, at any height  $z$ , the thickness  $h$  becomes comparable to the radial position  $R$ , the approximations are inappropriate.

It may be remarked, with the completion of the formulation of the one-layer theory for the eye wall, that proceeding to more highly resolved transverse structure is not a trivial extension. For example, proceeding to a two-layer model entails distinguishing the significant transverse variation of the pressure field in the Bernoulli equation pertinent to each sublayer. But the total head, the swirl, the streamwise velocity component, and the gravitational term could be the same for each of two comparably thick sublayers constituting the relatively thin eye wall, so such distinguishing requires subtlety. Multiple-subdivision analysis is not pursued here and attention is confined to the one-layer formulation.

If, in the one-layer formulation, one has the same thermodynamic stratification and angular-momentum stratification of the ambient, the same degree of flushing of the eye, and the same ratio of inflow-layer thickness to inflow-layer-separation distance for a fully developed eye ( $h_0^{*(i)}/r_0^{*(1)}$ ), then the only distinction in the dimensionless formulation between two cases (one of which conceivably could be a hurricane case and the other a tornado case, within the above constraints) is the dimensionless parameter  $\Sigma_3$  [ $\equiv (2g^*r_0^{*(1)})/(v^{*(1)})^2$ ], in that the radial scale to peak low-level wind position for a fully developed eye,  $r_0^{*(1)} \equiv r_1^*$ , might be quite different in the two cases. The parameter  $\Sigma_3$  enters in the gravitational term of the Bernoulli equation.

## 5. PRELIMINARY RESULTS

Results of the numerical computations are presented in Figures 8-10. Typical thermodynamic ambient data is analyzed for a hurricane environment [specifically, a typical West Indies environment for September (Jordan 1948)] and a tornado environment (unpublished sounding taken in Jackson, MS, April 1978, in spatial and temporal proximity of a moderate-intensity tornado). For each ambient profile, the thermodynamic variables (as functions of  $z^*$ ) characterizing the moist adiabat and eye region are calculated as described in Appendix A (see also Fendell 1974), as a prerequisite to the eye-wall calculation described in the previous section.

For both hurricane and tornado, under various adopted stratifications for the ambient circulation, the initial value of  $R$  (the outer edge of the eye wall at ground level,  $z = 0$ ) increases monotonically with an increase in the altitude to which the axial region (region IV, Figure 6) is filled with moist air. This result may be anticipated as follows: an increase of the height to which moist air persists in the nominally dry-adiabat eye region reduces the surface-level pressure deficit between the axis and the ambient. Reduction in pressure deficit results in a decrease of the peak swirl speed of the main vortex under the cyclostrophic approximation (4.16). It then follows, from the conservation of angular momentum, (4.24), that  $R$  increases.

For the hurricane ambient, the observed shape of the eye wall is significantly altered by the stratification (i.e., the change with altitude) of the angular momentum  $\Gamma$  at the periphery of the vortex (Figure 8). When this angular momentum is taken invariant with altitude [ $M \rightarrow \infty$  in (4.12)], the eye wall shape is seen to be nearly vertical at low altitude, followed at high altitude by a pronounced curvature radially outward into the ambient region I; the eye-wall position  $R$  increases with altitude  $z$  for higher values of  $z$ . As the depth of the moist-air layer at the base of the eye region increases [i.e., increasing  $i$  in (4.15)] the vertical portion of the eye-wall locus extends further up in the troposphere. For  $z_*^* = 0.5 z_c^*$  [see (4.15)], the locus terminates horizontally ( $R$  increasing at fixed  $z$ ) at an altitude about two-thirds of the distance to the tropopause. Here  $z_*^*$  is that cutoff height down to which the dry adiabat is extended from the tropopause, such that moist-adiabatic air

lies in  $z_{*}^{*} > z^{*} > 0$ ;  $z_{t}^{*}$  is the top of the tropopause, which, for the hurricane data, is computed to be approximately 45,000 feet. As more adiabatic air is flushed from the eye (i.e., for  $z_{*}^{*}$  decreasing), the termination altitude also decreases until, for an eye completely flushed of moist air so that  $z_{*}^{*} = 0$ , the termination altitude is only about one-fifth  $z_{t}^{*}$ .

If the angular momentum in the vortex is functionally prescribed to decrease to zero at  $z_{t}^{*}$ , a marked change in the computed eye-wall shape is noted. In general, the faster this decrease of  $\Gamma$  with altitude (i.e., the smaller  $M$  in (4.12)), the stronger is the tendency for the eye wall to penetrate radially toward the eye center. For  $M = 1$ , the "eye wall profiles" actually turn horizontally toward the vortex axis.

For the more moderate value  $M = 2$ , elongated "S" shaped profiles are produced. These eye-wall loci penetrate higher into the tropopause than both those for smaller values ( $M = 1$ ) and larger values ( $M \rightarrow \infty$ ). Indeed, for  $z_{*}^{*} = 0.5 z_{t}^{*}$  [i.e., for  $i = 6$  in (4.15)], the eye wall reaches the top of the tropopause ( $z \doteq 45,000$  ft). As discussed in the next section, future work will involve seeking to identify those angular-momentum stratifications which can yield a vertical eye-wall locus through the entire extent of the troposphere.

In Figure 9, the altitudinal variation of the eye-wall thickness  $h$ , the velocity component in a plane containing the axis of symmetry  $q$ , and the velocity component (swirl) in a plane perpendicular to the axis of symmetry  $v$ , are presented. The case examined is "unstratified" (i.e.,  $M \rightarrow \infty$ ), with the eye consisting of moist air from the ground up to  $z_{*}^{*} = 0.5 z_{t}^{*}$  [i.e.,  $i = 6$  in (4.15)]. The eye-wall thickness is found to increase monotonically with height. The theory is based on a thin eye wall, i.e.,  $h \ll R$  at all  $z$ , and indeed,  $h \leq 0.22$  throughout, while  $R \geq 1.7$  everywhere. The swirl velocity  $v$  is nearly constant at low altitude, then decreases at higher altitudes. This behavior follows directly from the radially outward bending of the eye-wall location  $R$ , since this particular case entails angular momentum  $\Gamma = R v = \text{const.}$

Results for the tornado ambient, Figure 10, exhibit a characteristically different solution. Here, for each of the angular-momentum-stratification parameters examined ( $M = 1, 2, \infty$ ), the completely dry eye ( $i = 1$ ) represents a "ceiling" solution for the eye-wall shape. That is, the eye-wall solution locus monotonically increases radially outward with increasing altitude and represents an upper bound such that, for a given  $M$ , resultant eye-wall loci for increasingly moist eyes do not penetrate much above this "ceiling" locus. As a deeper layer of moist air is taken to exist at the base of the eye region, i.e., as  $i$  increases from unity to larger values, the resultant eye wall loci rise from their surface-level values until they meet the "ceiling" solution at approximately  $x_*^*$ . They then roughly follow this ceiling solution radially outward, such that  $R$  increases to larger values.

Like the hurricane, the radial displacement  $R^*$  of the outside surface of the eye wall at the ground  $z^* = 0$  increases monotonically as additional moist-adiabatic air is added to the base of the dry-adiabat locus near the axis. Also, as the angular momentum of the peripheral vortex decreases more rapidly with height, i.e., as  $M \rightarrow 1$ , the eye wall shape "bends" more acutely toward the axis of rotation before intersecting the "ceiling" solution.

## 6. FUTURE DIRECTIONS

An inviscid axisymmetric nonentraining nonheat-conducting analysis of the eye wall in a two-cell vortex has been set forth. The flow exterior to the eye wall is a potential vortex, and the flow in the compressionally heated eye (interior to the eye wall) is static. Preliminary results suggest a key role for the variation of the angular momentum of the outer vortex  $\Gamma$  with altitude  $z$ , for perhaps only with a limited class of such stratifications can a two-cell structure be realized for a given convectively unstable ambient, with a fully developed (or fairly, well developed) eye and reasonable vortex dimensions. Very preliminary results suggest that a fairly vertical eye wall through an appreciable fraction of the troposphere is not achieved for outer-vortex angular momentum invariant with altitude. In fact, a useful exercise planned for the future is to take  $R$ , the eye-wall position relative to the axis of symmetry, fixed for all  $z$  at its low-level value for altitude  $z = 0$  and to use the resulting four previously-derived coupled nonlinear (now entirely algebraic) equations to obtain the eye-wall thickness  $h(z)$ , its streamwise speed,  $q(z)$ , its swirl speed  $v(z)$ , and  $\Gamma(z)$ ; hopefully for pertinent parametric input, this inverse problem [for which the conventional roles of  $\Gamma(z)$  and  $R(z)$  are reversed, in that now  $\Gamma(z)$  becomes an output and  $R(z)$  an input] has a solution over an extended range of altitude, say  $0.8 z_t > z > 0$ . A more difficult exercise would be to ascertain the  $\Gamma(z)$  for which the difference  $[R(z) - h(z)]$ , characteristic of the locus of the eye/eye-wall interface, is constant in  $z$  over much of the range  $z_t > z > 0$ . The statement possible at this early stage of investigation is that, for specified input (vortex parameters, ambient atmospheric sounding of the troposphere), the measurable quantity  $\Gamma(z)$  may be a means of ascertaining whether a one-cell moderate vortex can become a two-cell, intense vortex; in fact, no other candidate for a structure-differentiating observable seems readily identifiable.

Finally, some brief comments are appended concerning a longer-range plan of investigation, which incorporates dynamics in the eye, since the work discussed thus far is limited to a static description of the eye. It should suffice to state but once the obvious proviso that the direction of sequential investigations are heavily contingent on results of earlier investigations. It has already been mentioned that, upon adoption of a

family of very simple models of entrainment, one should investigate whether the steady supply of very-low-momentum fluid, entering the eye region (with sea-level enthalpy) from the much thinner, frictional sub-layer (under the more energetic, effectively nondiffusive outer portion of the inflow layer), is carried away by the entrainment process. If this is possible at the postulated eye pressure, then a geometry consistent with the postulated eye pressure arises.

Accordingly, one could adopt an initial condition in which the eye pressure is higher than that of the steady flow which emerges from the studies of the last paragraph, for one of the entrainment models. With that same entrainment model, with a quasi-steady treatment of the eye, and with no entrainment on the outside of the rising air in the (eye-wall) annulus, one could try to formulate and solve a one-spatial-coordinate, time-dependent model of the motion leading to time-description of eye development. By one-spatial-coordinate modeling, reference is being made to the same kind of transversely-averaged analysis as that executed earlier in this report. However, in the present context, the outer potential-vortex mass can migrate, inertially, and the proportions of "tropopause air" and sea-level air in the eye can change. The inertial migration refers to an oscillation established during the later stages of tropical-cyclone intensification, as radially-inward-moving particles overshoot their radial position of equilibrium (in which centrifugal acceleration is made compatible with moist-adiabatic-ascent-associated low-level pressure reduction from ambient value). The reconciliation during spin-up of the radial conservation of momentum (gradient-wind-type equation) and the axial conservation of momentum (hydrostatics) furnishes constraints discussed elsewhere by Carrier (1971a).

It is worth reiterating that experimental guidance for the entrainment models to be adopted is sorely needed, since in the present instance the occurrence of appreciable swirl in the fast-moving stream alters the situation from the more commonly encountered case, in which the fast-moving stream (contiguous to the slower-moving stream) is not rotating.

Only after the core region of intense atmospheric vortex is more in hand is examination of the upper-level outflow of mass, momentum, and energy from the typhoon, and its compatibility with the synoptic situation

in the far field, intended. The pressure deficit associated with the vortex cannot be maintained without such compatibility, but what the pressure deficit in fact may be cannot be ascertained without a better comprehension of the one-cell/two-cell transition in a tropical cyclone.

Finally, aside from matters of horizontal scale, of lifespan, and of enthalpy transfer at the surface, a particularly relevant distinction between the exceptional long-lived, long-path, high-swirl-speed tornado spawned by a rotating thunderstorm and the typhoon is the speed of translation of the two atmospheric systems. Hurricanes drift westward in the trades at about 15-20 mph, and, even in recurvature around persistent subtropical anticyclones, rarely translate much in excess of 35 mph. In contrast tornadoes often translate in the vicinity of 70 mph, and entail systems with strong vertical wind shear; i.e., the advective component of velocity in the vicinity of the midlatitudinal supercell changes magnitude and direction with altitude, whereas the absence of such "ventilation" is virtually a prerequisite for the intensification of tropical cyclones. The pertinence of the four-part structure of an intense atmospheric vortex presented for tropical cyclones may not suffice for the tornado cyclone; especially, the suitability of regarding the system as closed and containing its own "captured" airmass (throughput supply) of convectively unstable air (the large region I of the adopted four-part structure) is unclear.

TABLE 1. NUMERICAL RESULTS FOR EXTREMA OF THE TURNAROUND,  
FROM INTEGRATION OF THE INITIAL-VALUE PROBLEM (3.8)-(3.10).

$\alpha$	$\beta$	$\alpha/\beta$	$\bar{x}'(0) \approx \bar{x}'_0$	$(\bar{x}^-)_{calc}$	$(\bar{x}^-)_{\alpha=0}$	$(\bar{x}^+)_{calc}$	$(\bar{x}^+)_{\alpha=0}$
0.0	0.1	0.0	2.0	0.791	0.789	1.264	1.266
0.0	0.1	0.0	5.0	0.754	0.751	1.326	1.329
0.0	0.1	0.0	10.0	0.742	0.738	1.348	1.352
0.0	0.1	0.1	100.0	0.732	0.727	1.366	1.372
0.0	0.2	0.0	2.0	0.718	0.714	1.392	1.397
0.0	0.2	0.0	5.0	0.671	0.664	1.489	1.497
0.0	0.2	0.0	10.0	0.656	0.647	1.524	1.533
0.0	0.2	0.0	100.0	0.644	0.632	1.553	1.565
0.1	0.1	1.0	2.0	0.820	0.789	1.295	1.266
0.1	0.1	1.0	5.0	0.777	0.751	1.348	1.329
0.1	0.1	1.0	10.0	0.762	0.738	1.366	1.352
0.1	0.1	1.0	100.0	0.750	0.727	1.381	1.372
0.1	0.2	0.5	2.0	0.748	0.714	1.422	1.397
0.1	0.2	0.5	5.0	0.695	0.664	1.510	1.497
0.1	0.2	0.5	10.0	0.677	0.647	1.541	1.533
0.1	0.2	0.5	100.0	0.663	0.632	1.567	1.566
0.1	0.5	2.0	2.0	0.876	0.846	1.212	1.181
0.1	0.5	2.0	5.0	0.841	0.818	1.244	1.223
0.1	0.5	2.0	10.0	0.828	0.808	1.254	1.237
0.1	0.5	2.0	100.0	0.818	0.800	1.264	1.250
0.2	0.1	2.0	2.0	0.845	0.789	1.325	1.266
0.2	0.1	2.0	5.0	0.796	0.751	1.369	1.329
0.2	0.1	2.0	10.0	0.779	0.738	1.384	1.352
0.2	0.1	2.0	100.0	0.765	0.727	1.396	1.372
0.2	0.2	1.0	2.0	0.774	0.714	1.452	1.397
0.2	0.2	1.0	5.0	0.716	0.664	1.530	1.497
0.2	0.2	1.0	10.0	0.695	0.647	1.558	1.533
0.2	0.2	1.0	100.0	0.678	0.632	1.581	1.566
0.2	0.4	0.5	2.0	0.685	0.615	1.652	1.606
0.2	0.4	0.5	5.0	0.617	0.550	1.789	1.772
0.2	0.4	0.5	10.0	0.594	0.528	1.838	1.832
0.2	0.4	0.5	100.0	0.578	0.509	1.877	1.887

Notes: Results for  $(\bar{x}^\pm)_{\alpha=0}$  are from (3.17). Also,  $\bar{x}$  and  $\bar{x}'_0 = 100$  are within 2% of values for  $\bar{x}'_0 \rightarrow \infty$ , for  $\alpha, \beta$  studied.

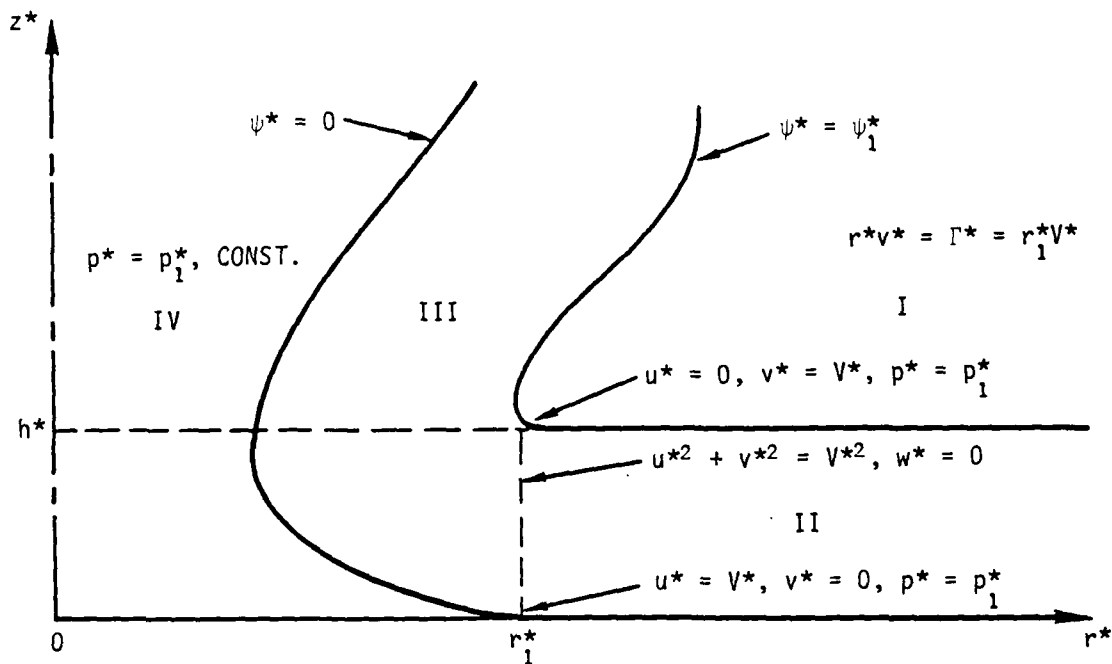


Figure 1. Schematic, not to scale, of an inviscid model of the turnaround region of a severe vertical quasisteady axisymmetric vortex. The "eye", region IV, is isobaric at pressure  $p_1^*$ , over the vertical extent of interest here, where  $p_1^*$  is also the pressure at  $r^* = r_1^*$ ,  $z^* = h^*$  (because the pressure above hydrostatic is approximately invariant across the surface inflow layer II). The "eye wall", region III, is demarcated by two streamsurfaces,  $\psi^*(r^*, z^*) = \text{const.}$  (the position of each to be determined), encompassing the mass efflux from region II. It is recalled that a potential vortex holds in region I.

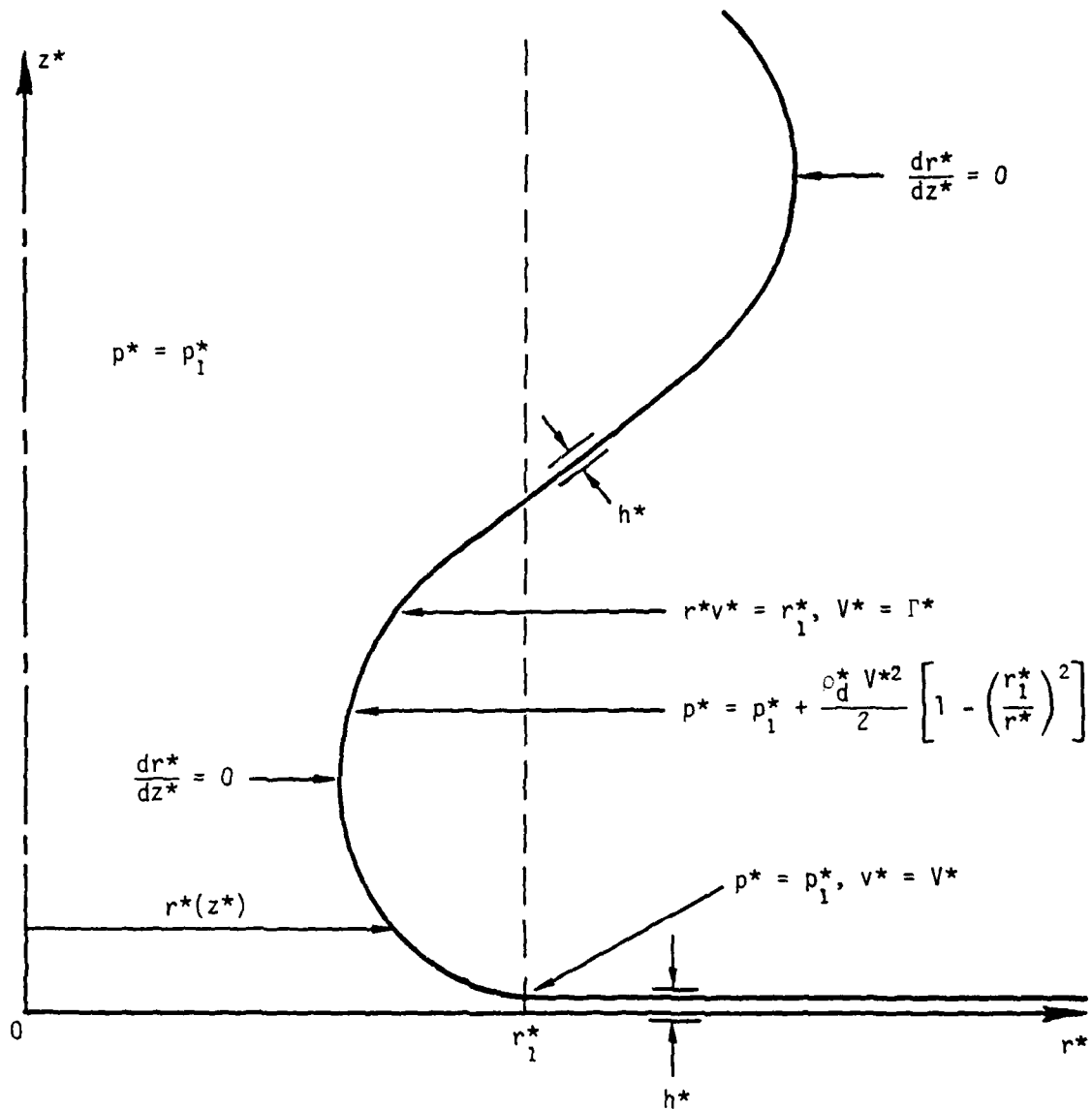


Figure 2. Schematic of the location of an inviscid "eye wall without structure" demarcating the interface between an isobaric nonswirling "eye" at pressure  $p_1^*$  and a potential vortex. The sheet representing the "eye wall" has thickness  $h^* \rightarrow 0$ ; in turnaround region, its displacement from the axis, as a function of height above the ground plane, is denoted  $r^*(z^*)$ .

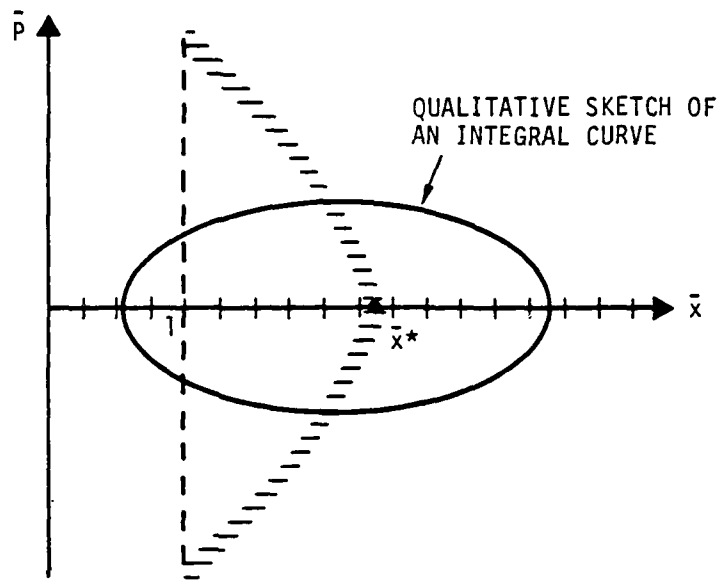


Figure 3. Phase-plane properties of equation (3.12), where  $\bar{p} = (d\bar{x}/d\bar{z})$ , with  $\bar{x}$  the dependent variable ( $\bar{x} > 0$ ) and  $\bar{z}$  the independent variable. Isoclines of zero and infinite slope are noted. At  $\bar{x} = 1$ , the distance from the axis of symmetry at which the surface inflow layer separates, a finite positive slope is adopted. For  $\alpha > 0$ ,  $\bar{x}_* > 1$ ; for  $\alpha = 0$ ,  $\bar{x}_* = 1$ . The sketched trajectory (solution curve) is a limit cycle (closed curve indicative of periodic behavior). The periodicity is not of physical interest.

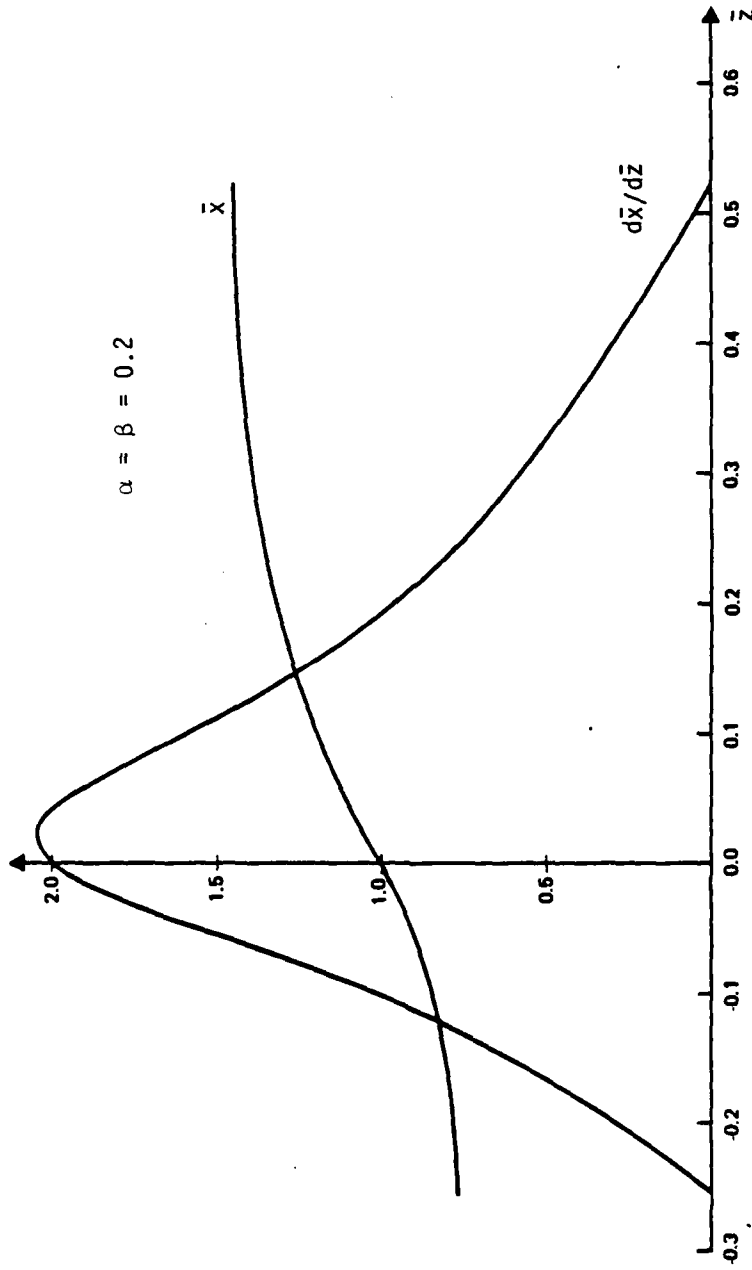


Figure 4. The solution to the boundary-value problem posed by equations (3.9), (3.10), and (3.12), for  $\bar{x}_0' = 2$ ; the solution may be completed by symmetry considerations to constitute a full cycle.

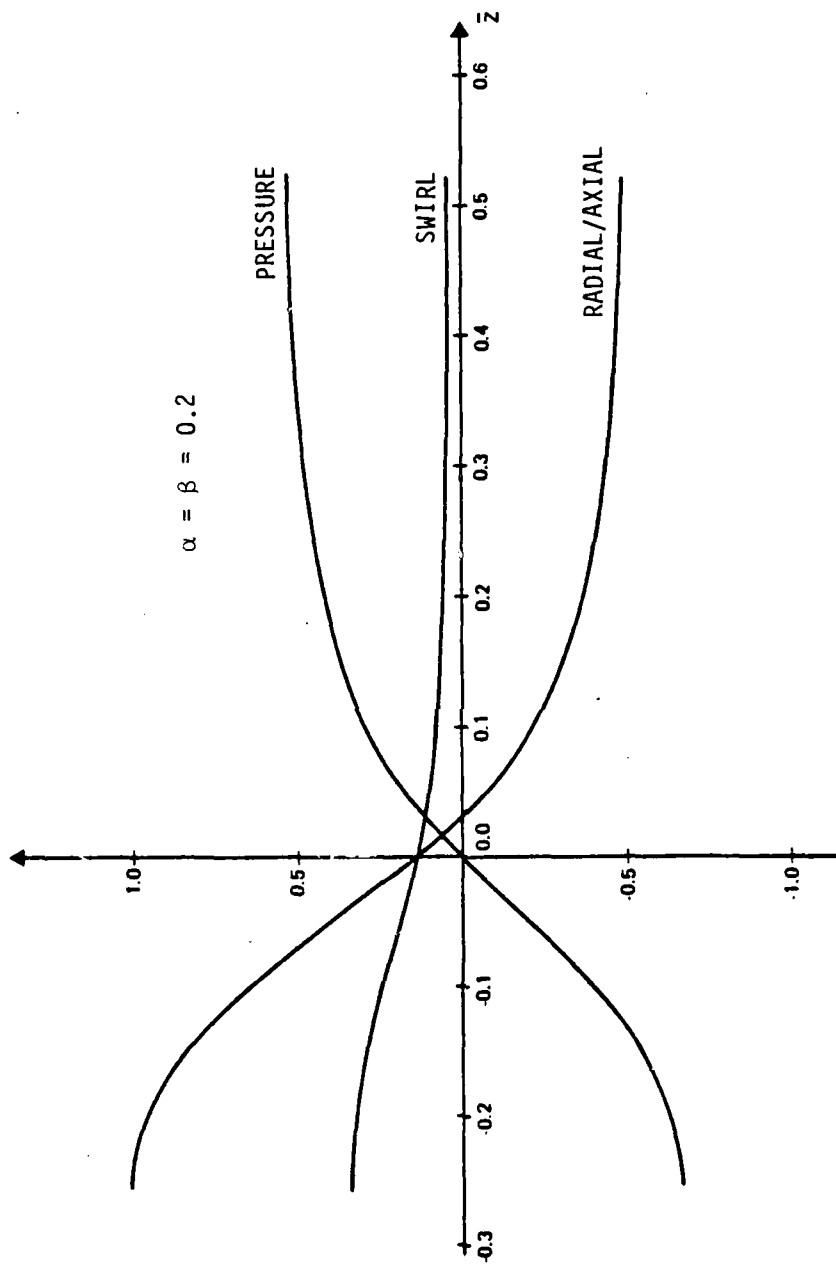


Figure 5. The solution to the boundary-value problem posed by equations (3.9), (3.10), and (3.12), for  $\alpha = 0.2$ ,  $\beta = 0.2$ , and  $\bar{x}'_0 = 2$ , given in Figure 4, is further studied. The "pressure" denotes the value of  $(1 - \bar{x}^{-2})$ ; the "swirl" denotes the value of  $\alpha \bar{x}^{-3} [1 + \bar{x}'^2]^{1/2}$ ; the "radial/axial" denotes the value of "swirl" minus "pressure", i.e., the left-hand side of (3.12).

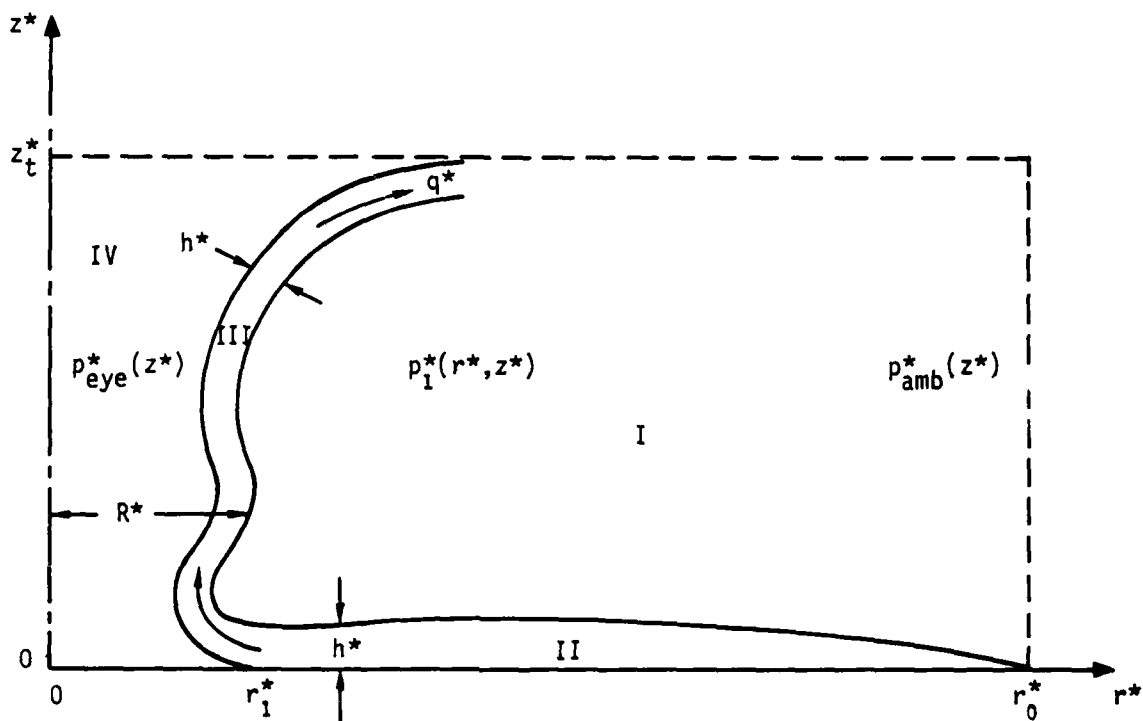


Figure 6. Another schematic of the postulated four-part model of the structure of a mature intense hurricane, of radial extent  $r_0^*$  and axial extent  $z_t^*$  (the tropopause). The potential vortex in region I is here ascribed axial variation, such that the associated pressure field is denoted  $p_1^*(r^*, z^*)$ , where  $p_1^*(r_0^*, z^*) = p_{amb}^*(z^*)$ , given. The low-level swirling influx (region II) grows in thickness, and separates to form the "eye wall" (region III) of thickness  $h^*$ ; the flow speed independent of swirling is denoted  $q^*$ . The pressure variation in the "eye", region IV, is entirely axial and is denoted  $p_{eye}^*(z^*)$ ; for the idealization of a completely dry, cloud-free, fully developed eye, this variation is determined by dry-adiabatic compression of tropopause-level air.

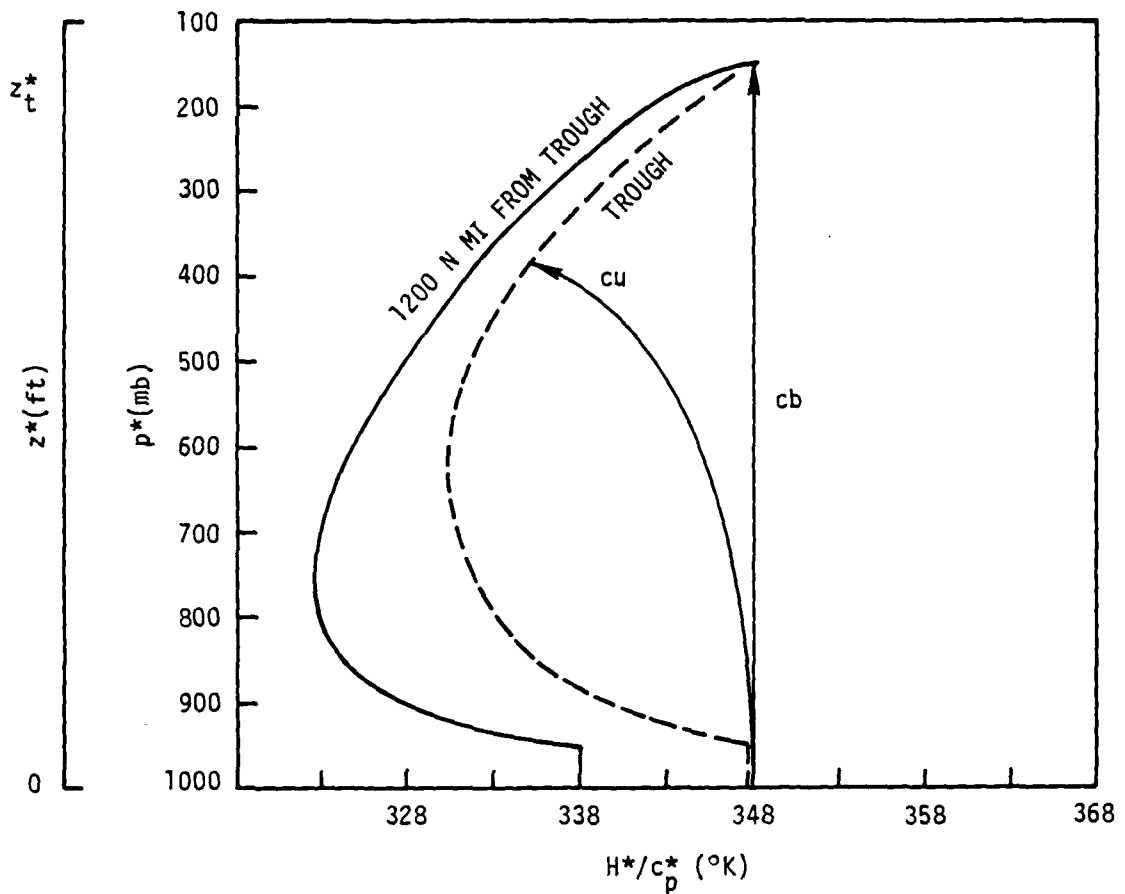


Figure 7. A typical profile of the total static temperature ( $H^*/c_p^*$ ) over the ocean in the equatorial trough and in the subtropics (1200 n mi from the equatorial trough), as a function of pressure  $p^*$  and altitude above sea-level  $z^*$  (Palmer and Newton 1970, p. 439, 575). The loci of thermodynamic states for a typical, relatively slowly rising cumulus (cu) and also for the undiluted core of a nonentraining, relatively rapidly rising cumulonimbus (cb) are also noted; the locus (cb) is that appropriate for moist-adiabatic ascent of sea-level air. The dashed curve is the typical ambient referred to in the text: a well-mixed lowest layer, a midtropospheric minimum, and a recovery of sea-level value at altitude  $z_t^*$  (defined here to be the tropopause, and typically about 50,000 ft). The quantity  $H^*$  is the sum of the static enthalpy, the latent heat equivalent of the water vapor present, and the gravitational potential energy; the quantity  $c_p^*$  is the specific heat at constant pressure, which may be taken to be effectively that of dry air.

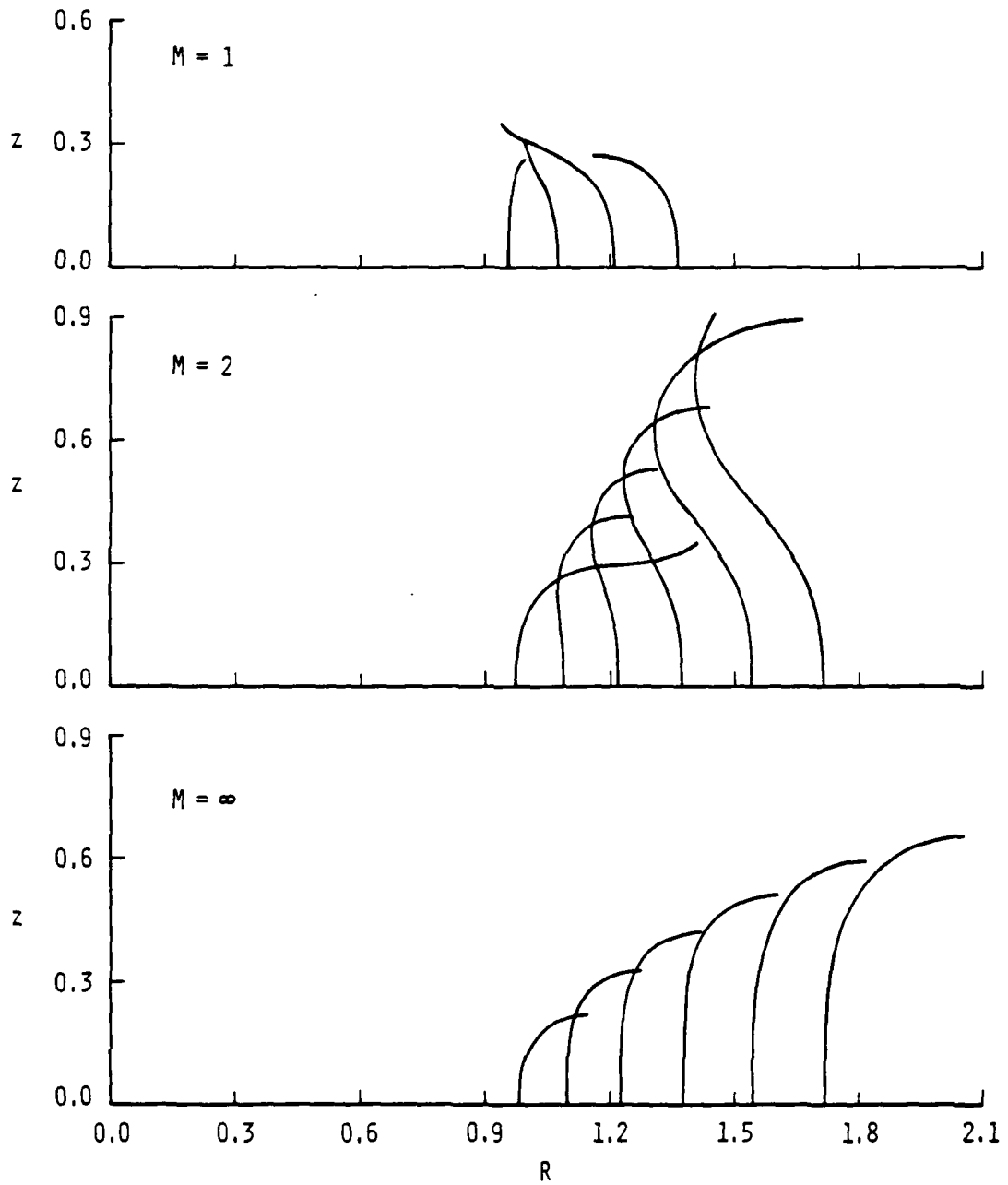


Figure 8. (Caption on Succeeding Page).

Figure 8. The outer edge of the eye wall,  $R$ , measured from the center of the potential vortex, is presented as a function of altitude,  $z$ , for a hurricane environment. Here  $R$  and  $z$  are nondimensionalized by  $r_1^* = 50,000$  ft. Cases are presented for three different values of the angular momentum "stratification" parameter  $M$  in (4.12), namely  $M = 1, 2,$  and  $\infty$ . For each case, the eye wall locus closest to the axis (i.e., the locus with smallest  $R$  at  $z = 0$ ), represents an eye region completely flushed of moist air [i.e.,  $i = 1$  in (4.15)]. Successive loci at larger radial positions represent eyes increasingly filled with moist air, specifically unity increases of  $i$  in (4.15).

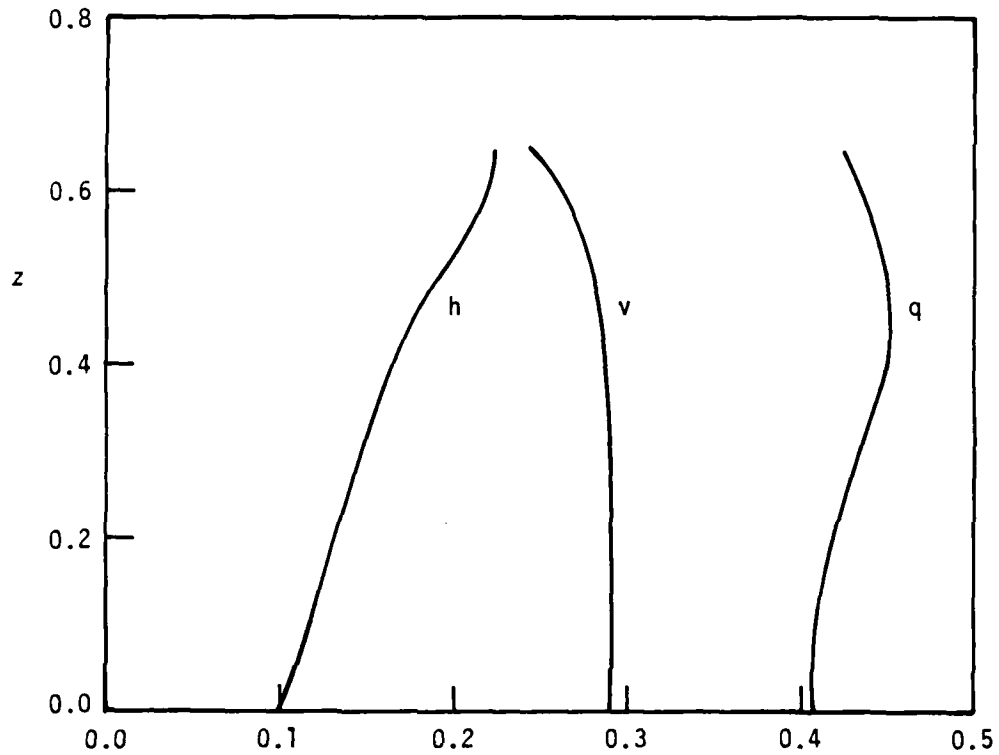


Figure 9. For a hurricane environment, the altitudinal variation of the eye wall thickness  $h$ , the velocity component in a plane containing the axis of symmetry  $q$ , and the velocity component in a plane perpendicular to the axis of symmetry  $v$ , are presented. The case examined is "unstratified" ( $M \rightarrow \infty$ ), with the eye consisting of moist air from the ground up to  $z_*^* = 0.5 z_t^*$  [i.e.,  $i = 6$  in (4.15)], where  $z_t^*$  is the top of the tropopause. Here  $h$  is nondimensionalized by  $r_1^* = 50,000$  ft, while  $q$  and  $v$  are nondimensionalized by  $v^{*(1)} = 422.9$  ft/sec.

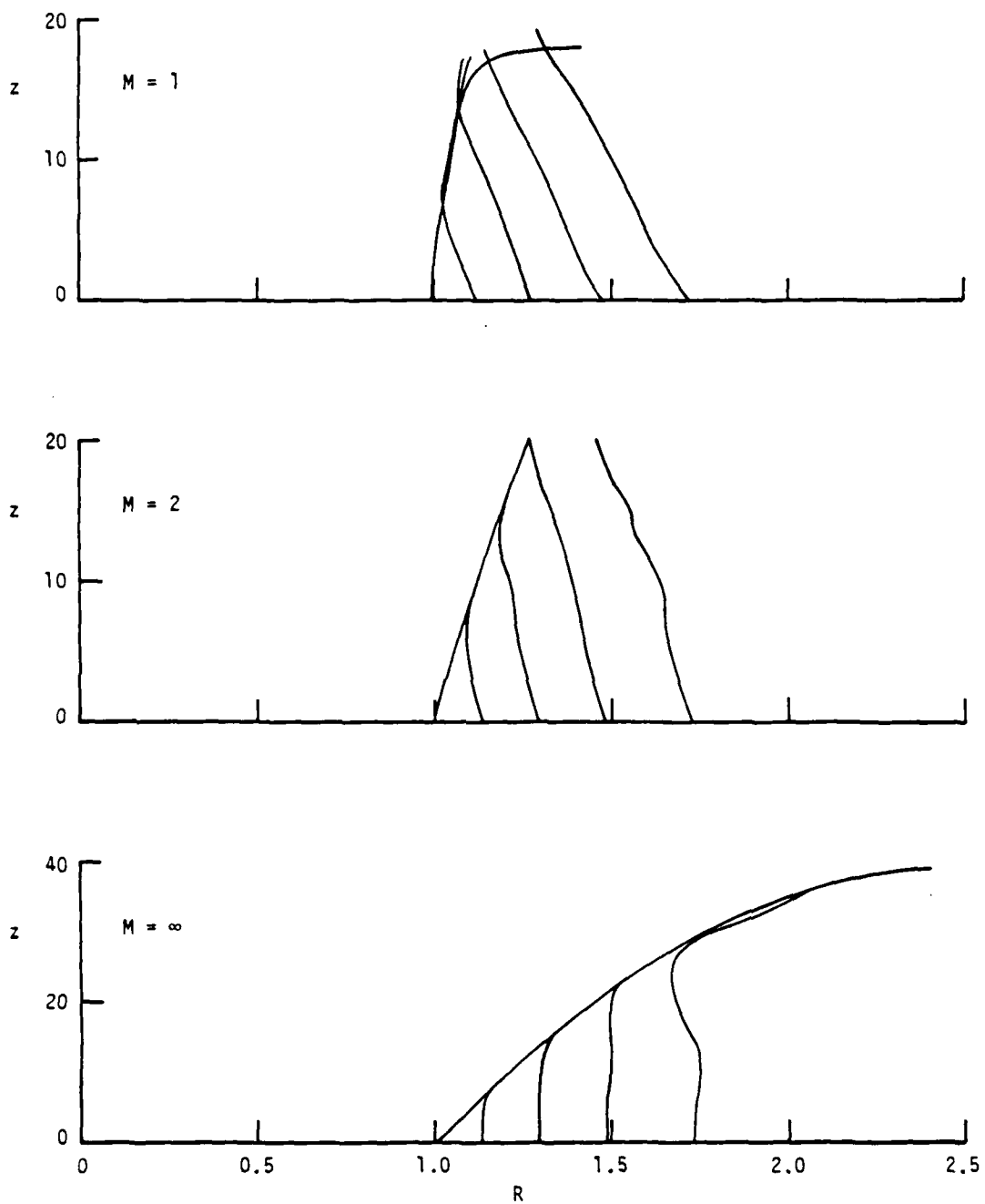


Figure 10. In a similar manner to Figure 8, but for a tornado environment, the radial edge of the eye wall  $R$  is presented as a function of altitude  $z$ . Here  $R$  and  $z$  are nondimensionalized by  $r_1^* = 500$  ft.

## REFERENCES

- Batchelor, G. K. (1967). An Introduction to Fluid Dynamics. Cambridge, England: Cambridge University.
- Brand, S., Chambers, R. P., Woo, H. J. C., Cermak, J. E., Lou, J. J. and Danard, M. (1979). A preliminary analysis of mesoscale effects of topography on tropical cyclone-associated surface winds. NAVENVPREDRSCHFAC Technical Report TR 79-04. Monterey, CA: Naval Environmental Prediction Research Facility.
- Burggraf, O. R., Stewartson, K. and Belcher, R. (1971). Boundary layers induced by a potential vortex. *Phys. Fluids* 14, 1821-1833.
- Carrier, G. F., Dergarabedian, P. and Fendell, F. E. (1979). Analytic studies on satellite detection of severe, two-cell tornadoes. Contractor Report 3127. Washington, DC: National Aeronautics and Space Administration.
- Carrier, G. F. and Fendell, F. E. (1978). Analysis of the near-ground wind field of a tornado with steady and spatially varying eddy viscosity. Wind Field and Trajectory Models for Tornado-Propelled Objects (EPRI Project 308, Report NP-748), pp. A-1 - A-45. Palo Alto, CA: Electric Power Research Institute.
- Carrier, G. F., Hammond, A. L. and George, O. D. (1971). A model of the mature hurricane. *J. Fluid Mech.* 47, 145-170.
- Carrier, G. F. (1970). Singular perturbation theory and geophysics. *SIAM (Soc. Industr. Appl. Math.) Rev.* 100, 451-560.
- Carrier, G. F. (1971a). The intensification of hurricanes. *J. Fluid Mech.* 49, 145-158.
- Carrier, G. F. (1971b). Swirling flow boundary layers. *J. Fluid Mech.* 49, 133-144.
- Fendell, F. E. (1974). Tropical cyclones. Advances in Geophysics, Vol. 17, pp. 1-100. New York: Academic.
- Gray, W. M. (1979). Tropical cyclone origin, movement and intensity characteristics based on data compositing techniques. NAVENVPREDRSCHFAC Contractor Report CR 79-06. Monterey, CA: Naval Environmental Prediction Research Facility.
- Hall, M. G. (1972). The structure of vortex breakdown. *Ann. Rev. Fluid Mech.* 10, 221-246.
- Jordan, C. L. (1957). A mean atmosphere for the West Indies area. National Hurricane Research Project Report No. 6. Washington, DC: U.S. Department of Commerce.

- Launder, B. E. (1964). Laminarization of the turbulent boundary layer in a severe acceleration. *J. Appl. Mech.* 31, 707-708.
- Leibovich, S. (1978). The structure of vortex breakdown. *Ann. Rev. Fluid Mech.* 10, 221-246.
- Lewellen, W. S. (1977). Theoretical models of the tornado vortex. Proceedings of the Symposium on Tornadoes: Assessment of Knowledge and Implications for Man, R. E. Peterson, ed., pp. 107-143. Lubbock, TX: Institute for Disaster Research, Texas Tech University.
- Maikus, J. S. and Riehl, H. (1960). On the dynamics and energy transformation in steady-state hurricanes. *Tellus* 12, 1-20.
- Palmen, E. and Newton, C. W. (1969). Atmospheric Circulation Systems. New York: Academic.

## APPENDIX A. A DERIVATION OF THE MOIST ADIABAT

Consider a volume  $V$  with surface  $S$  and surface element  $dS$ ; the outward normal vector to  $dS$  is denoted  $n_i$  and fluid velocity vector is denoted  $u_i$ . Super asterisks, used in the main text to denote dimensional quantities, are dispensed with for this appendix.

For conservation of mass, consider air first. The flux of dry air through  $dS$  is in Cartesian notation,  $\rho u_i n_i dS$ , where  $\rho$  is air density. Hence, in the steady state,

$$\oint_S \rho u_i n_i dS = 0 \Rightarrow (\rho u_i)_{,i} = 0, \quad (\text{A.1})$$

where comma denotes partial differentiation. Water vapor has the same speed, but density  $\sigma$ . When  $\sigma < \Sigma(T)$ , where  $\Sigma(T)$ , the saturation vapor density, is a known function of the temperature  $T$ ,

$$(\sigma u_i)_{,i} = 0.$$

If the mixing ratio for water vapor  $Y \equiv \sigma/\rho$ , then

$$\rho u_i Y_{,i} = 0. \quad (\text{A.2})$$

When  $T$  is low enough,

$$\sigma = \Sigma(T). \quad (\text{A.3})$$

For conservation of momentum, the momentum flux associated with  $u_i$  is  $(\rho + \sigma)u_j n_j u_i dS$ , and that associated with the partial pressure of air  $p$  and with the partial pressure of vapor  $\alpha$  is  $(\alpha + p)n_i dS$ . The production of momentum per unit volume associated with the gravitational body force ( $g$  is the magnitude of the acceleration of gravity) is  $-g z_{,i}(\rho + \sigma)$ , where the spatial coordinate  $z$  lies parallel to the body force. The loss of momentum per unit volume associated with the disappearing fluid is  $-(\sigma u_j)_{,j} u_i$ . Thus, using (A.1),

$$\oint_S (\rho + \sigma) u_j n_j u_i dS + \oint_S (\alpha + p) n_i dS = -g \int_V (\rho + \sigma) z_{,i} dV + \int_V (\sigma u_j)_{,j} u_i dV \quad (A.4)$$

becomes

$$(\rho + \sigma) u_j u_{i,j} + (\alpha + p)_{,i} + (\rho + \sigma) g z_{,i} = 0. \quad (A.5)$$

Incidentally, if a momentum equation had been written for each constituent, dry air and water vapor, interparticle drag of the form  $D = A(u_i - v_i)$  would have been introduced, where  $u_i$  is air velocity and  $v_i$  is vapor velocity, and here  $A \rightarrow \infty$  so  $v_i = u_i$ .

The equations of state are

$$p = \rho R T, \quad (A.6)$$

$$\alpha = \sigma R' T, \quad (A.7)$$

where the gas constant for vapor  $R'$  is related to the gas constant for vapor by  $R' = R/(m_v/m_a)$ , where  $m_v$  is the molecular weight of water vapor and  $m_a$  is the molecular weight of dry air.

The nonmechanical energy carried by the vapor can be written as  $(L_0 + c_v^v T)$ , where  $L_0$  is the (extrapolated) value of the heat of condensation at  $T = 0$ , and  $c_v^v$  is the specific heat at constant volume of the vapor  $v$ . With this description, the net heat released by condensation at temperature  $T$  would be

$$L = L_0 + (c_v^v - c)T, \quad (A.8)$$

where  $c$  is the specific heat of liquid water. The flux of energy across  $dS$  via  $u_i$  is

$$\left[ \rho u_i \left( c_v T + \frac{v^2 + q^2}{2} \right) + \sigma u_i \left( c_v^v T + \frac{q^2 + v^2}{2} + L_0 \right) \right] n_i dS, \quad (\text{A.9})$$

where  $c_v$  is the specific heat at constant volume of dry air. The stream-wise velocity component is denoted  $q$  and the perpendicular velocity component (swirl) is denoted  $v$ . Below,  $Q^2 \equiv (v^2 + q^2)$ . The work done by pressure forces across  $dS$  is  $(\alpha + p)u_i n_i dS$ , and the flux of potential energy is  $(\rho + \sigma)g z n_i u_i dS$ . The rate at which energy goes into a sink (i.e., into liquid, which, by conventional approximation in treating the moist adiabat, just vanishes) is the product of two factors:  $-(\sigma u_j)_{,j}$ , the rate of loss of mass per unit volume, and  $\left\{ g z + \left[ (q^2 + v^2)/2 \right] + c T \right\}$ . It follows that

$$\begin{aligned} & \left[ \rho u_j \left( c_v T + \frac{Q^2}{2} \right) + \sigma u_j \left( c_v^v T + L_0 + \frac{Q^2}{2} \right) + (\rho + \sigma)u_j g z + (\alpha + p)u_j \right]_{,j} \\ & = (\sigma u_i)_{,i} \left( c T + \frac{Q^2}{2} + g z \right). \end{aligned} \quad (\text{A.10})$$

Hence,

$$\begin{aligned} & \rho u_j \left( g z + \frac{Q^2}{2} \right)_{,j} + (\sigma u_j)_{,j} \left[ \left( c_v^v - c \right) T + L_0 \right] \\ & + \sigma u_j \left( c_v^v T + \frac{Q^2}{2} + g z \right)_{,j} + \rho u_j (c_v T)_{,j} \\ & + \left( u_j p_{,j} + p u_{j,j} \right) + \left( u_j \alpha_{,j} + \alpha u_{j,j} \right) = 0, \end{aligned} \quad (\text{A.11})$$

where  $(\sigma u_j)_{,j} = \rho u_j Y_{,j}$ ,  $\sigma u_j = \rho Y u_j$ , and the last line in (A.11) is

$$\rho u_j \left( \frac{p}{\rho} \right)_{,j} + \rho u_j \left( \frac{\alpha}{\rho} \right)_{,j}. \quad (\text{A.12})$$

Thus, since  $(c_v + R) = c_p$  and  $(c_v^V + R') = c_p^V$ ,

$$\begin{aligned} \rho u_j (1 + Y) \left( g z + \frac{Q^2}{2} \right)_{,j} + \rho u_j (c_p T)_{,j} + \rho u_j Y_{,j} (L_0 - c T) \\ + \rho u_j (Y c_p^V T)_{,j} = 0, \end{aligned} \quad (\text{A.13})$$

where  $c_p^V$  (not  $c_p^V$ ) appears because work is done on condensing gas and the enthalpy release is  $[L_0 - (c - c_p^V)T]$ . But

$$\rho u_j \left\{ (1 + Y) \left[ (Q^2/2) + g z \right]_{,j} + \frac{(p + \alpha)_{,j}}{\rho} \right\} = 0, \quad (\text{A.14})$$

so, if  $s$  is distance along a streamline, and since

$$Q \frac{\partial}{\partial s} = u_j \frac{\partial}{\partial x_j}, \quad (\text{A.15})$$

$$\frac{(\alpha + p)_{,s}}{\rho} - Y_{,s} (L_0 - c T) - (c_p T + Y c_p^V T)_{,s} = 0. \quad (\text{A.16})$$

If it is recalled that

$$\alpha = \Sigma(T) R' T, \quad \rho = p/R T, \quad Y = \Sigma(T) R T/p, \quad (\text{A.17})$$

the last equation becomes, if  $\bar{p} \equiv (p + \alpha)$  and  $\sigma \equiv (m_v/m_a)$ ,

$$\frac{d T}{d \bar{p}} = \frac{\frac{R T}{\bar{p} - \Sigma(T)} + [L_0 - (c - c_p^V)T] \frac{\sigma \Sigma(T)}{[\bar{p} - \Sigma(T)]^2}}{\left[ c_p + \frac{\sigma \Sigma(T) c_p^V}{\bar{p} - \Sigma(T)} \right] + [L_0 - (c - c_p^V)T] \frac{\sigma \bar{p} \Sigma'(T)}{[\bar{p} - \Sigma(T)]^2}}, \quad (\text{A.18})$$

where  $\Sigma'(T)$  denotes the first derivative, and all specific heats have been taken as constant. In some more approximate derivations,  $\bar{p} \doteq p$ ,  $(c_p + Y c_p^V) \doteq c_p$ , and  $c_p \doteq c_p^V$  in the first term of the denominator.

**DAT  
FILM**